In Silico Models of Aerosol Delivery to the Respiratory Tract – Development and Applications

P. Worth Longest[1,2] and **Landon T. Holbrook**[1]

[1]Department of Mechanical Engineering Virginia Commonwealth University, Richmond, VA

[2]Department of Pharmaceutics Virginia Commonwealth University, Richmond, VA

Abstract

This review discusses the application of computational models to simulate the transport and deposition of inhaled pharmaceutical aerosols from the site of particle or droplet formation to deposition within the respiratory tract. Traditional one-dimensional (1-D) whole-lung models are discussed briefly followed by a more in-depth review of three-dimensional (3-D) computational fluid dynamics (CFD) simulations. The review of CFD models is organized into sections covering transport and deposition within the inhaler device, the extrathoracic (oral and nasal) region, conducting airways, and alveolar space. For each section, a general review of significant contributions and advancements in the area of simulating pharmaceutical aerosols is provided followed by a more in-depth application or case study that highlights the challenges, utility, and benefits of *in silico* models. Specific applications presented include the optimization of an existing spray inhaler, development of charge-targeted delivery, specification of conditions for optimal nasal delivery, analysis of a new condensational delivery approach, and an evaluation of targeted delivery using magnetic aerosols. The review concludes with recommendations on the need for more refined model validations, use of a concurrent experimental and CFD approach for developing aerosol delivery systems, and development of a stochastic individual path (SIP) model of aerosol transport and deposition throughout the respiratory tract.

Keywords

Respiratory drug delivery; pharmaceutical aerosols; aerosol deposition; lung models; 1-D models; CFD models; spray momentum; targeted aerosol delivery; validation of deposition simulations; stochastic individual path (SIP) model

1. Introduction

Modeling respiratory aerosol delivery requires an analysis of transport and deposition in the respiratory tract as well as an understanding of dynamics within the aerosol generation device, which often influence the flow field and deposition characteristics in the upper airways. Numerical models of particle deposition in the lungs were initially developed in the context of assessing the dosimetry of inhaled environmental and occupational pollutants,

*Dr. P. Worth Longest, PhD (Corresponding author), Virginia Commonwealth University, 401 West Main Street, P.O. Box 843015, Richmond, VA 23284-3015, Phone: (804)-827-7023, Fax: (804)-827-7030, pwlongest@vcu.edu.

such as coal dust, cigarette smoke, and radionuclides. Decades of research on respiratory aerosol dosimetry were compiled in the ICRP [1, 2] and NCRP [3] documents and corresponding models. Over time, these whole-lung dosimetry models, which were developed for ambient monodisperse particles, were expanded and applied to better understand the deposition of pharmaceutical aerosols in the airways [4]. *In silico* model results generally agreed well with *in vivo* studies for upper (fast clearance) and lower (slow clearance) deposition fractions with stable monodisperse particles. However, these early whole-lung deposition models did not account for factors specific to respiratory drug delivery, such as inhaler spray momentum, droplet size change with dissolved solutes, and did not predict localized aerosol deposition. The advancement of computational fluid dynamics (CFD) technology has led to an alternative approach for dosimetry modeling in which aerosol transport and deposition is calculated from first principles in realistic three-dimensional (3-D) models of the inhaler and respiratory tract. CFD simulations can directly capture factors such as inhaler spray momentum [5], spray burst effect [6], turbulent inhaler jets [7], and droplet evaporation or hygroscopic growth [8, 9]. Recent comparisons of CFD model predictions to *in vivo* [10] and *in vitro* [11, 12] data show good agreement. As a result, applications of CFD models are progressing beyond providing an understanding of aerosol deposition mechanics and toward serving as an effective design and optimization tool for improving respiratory drug delivery. In this introductory section, types of numerical models are reviewed, advantages of CFD simulations are presented, and challenges related to the numerical modeling of respiratory aerosols are highlighted. This review then focuses on studies that contributed to the development of respiratory delivery models along with studies that applied these models to improve existing devices, target aerosol delivery to the lungs, and propose new aerosol delivery approaches.

1.1. Types of Respiratory Delivery Models

Current whole-lung models of aerosol dosimetry in the respiratory tract typically account for deposition within individual sections of the airways using physical or empirical correlations. The individual sections considered may range in scale from general regions of the lungs, like the tracheobronchial airways, down to individual airway branches. However, only penetration depth into the lungs is considered in the most detailed of these simulations, such that they are often referred to as one-dimensional (1-D) models. Correlations for deposition may be dependent upon individual transport mechanisms (such as diffusion, sedimentation, and impaction) as reviewed by multiple previous studies [13, 14], or may be empirically based [15, 16]. While these models are generally developed for monodisperse ambient aerosols, studies have advanced their utility to evaluate the effects of size change [17, 18], aerosol charge [19] and aerosol polydispersity [20]. Recently, *in vitro* experiments and CFD simulations were used to develop an empirical correlation for dry powder inhaler (DPI) deposition in the mouth-throat region as a function of jet and airway characteristics [7]. A similar correlation is not available for spray aerosols produced by metered dose inhalers (MDIs) and softmist inhalers. Recent advances in whole-lung respiratory dosimetry models and the underlying correlations were reviewed by Finlay and Martin [16]. The related online Respiratory Deposition Calculator of the Aerosol Research Laboratory of Alberta provides a convenient method to calculate the whole-lung deposition of pharmaceutical aerosols. The multiple path particle deposition model (MPPD) provided by the Hamner Institutes for Health Sciences and described by Asgharian et al. [21] is also a useful whole-lung modeling tool that can provide estimates of delivery to individual airway branches.

Strengths of 1-D whole-lung models are ease of use and the fact that deposition can be estimated throughout the respiratory tract. One disadvantage of these methods is that the available correlations may not cover all mechanisms related to pharmaceutical aerosol delivery from multiple platforms. A second disadvantage of these models is that the site of

deposition is not well described; that is, deposition is predicted in general regions such as the mouth-throat or tracheobronchial airways. In general, 1-D models neglect the geometric complexity of the airways along with the associated complex flow physics, such that these models cannot directly capture a number of phenomena known to influence particle deposition.

In contrast with 1-D models, modern CFD simulations calculate flow and aerosol physics based on first principles in 3-D sections of the inhaler and respiratory tract. The flow field is determined using a solution of the Navier Stokes equations which may include approximations for turbulence, compressible flow, and heat/mass transfer [22, 23]. The discrete particle or droplet phase is typically solved using Newton's second law accounting for all relevant forces acting on the discrete elements, such as drag, gravity, and Brownian motion, as well as heat and mass transfer with the continuous phase [9, 24, 25]. Recent studies have also developed very efficient models of particle motion using a continuous phase approach [26–28]. Simulations are conducted in idealized [29], patient specific [30], or characteristic models of the respiratory tract [31], as described later in this review.

A primary strength of CFD simulations is the use of general governing transport equations, such that the model can be applied to a wide range of airway geometries, aerosol conditions, and delivery devices without the need to develop empirical or semi-empirical deposition correlations. The CFD model provides a detailed description of the flow field at millions of representative points (control volume centers and nodes) and can predict deposition at very localized (sub-millimeter) levels [32–34]. Weaknesses of CFD simulations are the complexity of the computational model and the required computational time. More efficient CFD simulations of aerosol transport and deposition are an area of active research [25, 26]. Due to computational constraints, CFD simulations are currently limited to segments of the respiratory tract. However, the size of these regions that can be considered is increasing as computer resources continue to expand [35–37].

1.2 Model Selection

Considering the simulation of respiratory aerosol delivery, the type of model needed (1-D vs. 3-D CFD) depends on the analysis that is being performed. For cases in which adequate correlations exist and deposition is only required to be known in general regions, e.g., the mouth-throat and lungs, then 1-D models or correlations are often sufficient. Furthermore, CFD models are currently being used to expand the capabilities of 1-D whole-lung simulations. For example, Xi and Longest [31] developed a correlation for nanoparticle deposition in the nasal airways that can be integrated into a more complete 1-D model prediction of total respiratory tract dose. In contrast, CFD simulations are required when insufficient correlations are available and when information regarding local deposited dose is required. Knowledge of local deposited dose is often important in order to predict particle dissolution, transport through the mucus, and uptake at the cellular level [32, 38–40]. Moreover, the details provided by CFD simulations are often useful for not only understanding the performance of respiratory delivery systems, but also for optimizing system performance [41, 42] and designing new delivery devices and protocols [10, 43]. As a result, CFD simulations may often be the preferred numerical method for advancing the design of respiratory aerosol delivery systems and will be the focus of this review. However, 1-D models will also be considered to highlight the utility of this numerically efficient approach.

1.3 Challenges in Simulating Respiratory Aerosols

The simulation of even monodisperse ambient aerosols in the respiratory tract presents a number of challenges. Inhaled ambient aerosols can be defined as particles or droplets that

do not contain a drug and have no initial spray or jet momentum associated with an inhaler device or aerosol formation. Effective simulations must address complexities associated with the respiratory tract geometry, flow field, and aerosol physics. The respiratory tract is a dynamic structure spanning length scales from approximately 4 cm at the widest point of the oral cavity to approximately 300 μm in the alveolar region [44]. Transitional and turbulent flows often occur in the mouth-throat and upper conducting airways [12, 45, 46] whereas laminar viscous-dominant flow controls transport beyond approximately the 9th respiratory generation [36]. Within this wide range of conditions, aerosol deposition may occur due to impaction, sedimentation, diffusion, and turbulent dispersion based on particle size in conjunction with the local flow dynamics. Ambient aerosols may evaporate or condense within the warm and humid environment of the respiratory tract. Additional factors affecting the transport and deposition of these particles or droplets include charge [47], coagulation [48], and number density effects, like cloud motion [39]. Despite these complexities, a number of studies have shown good agreement between model predictions of ambient aerosol deposition in the respiratory tract and experiments. 1-D whole-lung models have been shown to match available *in vivo* results for upper airway (fast clearance) and lower airway (slow clearance) deposition for decades [1, 3, 21, 49–51]. CFD models of ambient particle and droplet deposition have also shown good agreement with deposition in specific airway regions, such as the mouth-throat [31, 52] and upper tracheobronchial airways [45, 53, 54], as discussed later in this review.

Pharmaceutical aerosols typically contain multiple compounds, including a drug, and may be associated with jet or spray momentum arising from the process of aerosol formation and flow through the device. In addition to the complexities associated with ambient aerosols, simulations of pharmaceutical aerosols must also consider the hygroscopic growth or evaporation of multicomponent droplets or particles and inlet flow conditions associated with the inhaler. For MDIs, significant evaporation of the initial spray droplets occurs and flow near the actuator nozzle is compressible, temperature dependent, and supersonic resulting in a high momentum turbulent spray jet entering the mouth-throat geometry [55]. For dry powder inhalers (DPIs), the aerosol often enters the mouth in a high speed turbulent jet, which is known to affect deposition [7] and particle deaggregation [56]. Hygroscopic growth may also be important for many dry powder aerosols. Soft mist inhalers reduce spray momentum effects; however, jets associated with aerosol formation and the inhaler mouthpiece may still significantly influence deposition [11, 57]. Considering model comparisons with experiments for pharmaceutical aerosols, DeHaan and Finlay [7] developed a correlation for the mouth-throat deposition of DPI aerosols as a function of jet diameter and inhalation flow rate, which was shown to match *in vivo* deposition data very well [16, 58]. CFD simulations of pharmaceutical aerosol delivery have been shown to match *in vitro* experiments for MDIs [10, 55], DPIs [12], and softmist inhalers [11, 57].

1.4 Challenges in Applying CFD Models

While CFD simulations provide advantages to predicting the fate of inhaled pharmaceutical aerosols, they are highly complex due to the underlying physics that must be captured. Challenges to CFD modeling of respiratory aerosols include the need for simulating turbulent and transitional flows, which may be compressible and supersonic near the site of droplet formation, as well as accounting for multiple phases, heat and mass transfer between multiple phases, transient inhalation waveforms, and motion of the airway geometry. Simulating turbulence presents a significant challenge to computational models [59]. Highly complex large eddy simulations have recently shown good agreement with empirical data for flow field dynamics and particle deposition during steady state inhalation [12, 60–63]. However, simpler and more numerically efficient two-equation k-ω models have also shown excellent agreement with *in vitro* data for the deposition of ambient and pharmaceutical

aerosols in inhalers and in the respiratory tract [5, 6, 42, 45, 57, 64]. Recent simulations have approximated the highly complex flow dynamics around spray nozzles during MDI and softmist aerosol formation including supersonic compressible flow and accurately predicted deposition in the upper respiratory airways [11, 55, 57]. Both 1-D [17, 18] and 3-D [43] models have been used to effectively predict the hygroscopic growth of pharmaceutical aerosols, which requires simulations of heat and mass transfer in both the discrete and continuous phases. Recent studies have also investigated the effects of geometry motion on flow field dynamics and aerosol deposition [65]. In general, the numerical model selected should be adequately complex to accurately capture the variables of interest, i.e., aerosol transport and deposition, yet as simple as possible to remain numerically efficient. Due to the complexities associated with modeling pharmaceutical aerosols and the very large number of potential simulation options, validation with experimental results is critical for effective model development.

For respiratory aerosols in general, numerical predictions often report deposition values on scales smaller than available experimental data. A large number of 1-D models predict branch-average data throughout the entire tracheobronchial tree. However, *in vivo* deposition data is typically limited to general regions (e.g., upper and lower airways) or shell regions of a lung volume [39]. Similarly, a large number of CFD studies report highly localized hot spots of deposition on sub-millimeter scales [27, 32–34, 66]. A relatively small subset of these studies have validated their results with branch-averaged or sub-regional values generated from *in vitro* experiments [12, 29, 67–71]. Other studies have considered qualitative validations by comparisons to local maps of deposition [70]. However, Longest and Vinchurkar [72] have shown that respiratory bifurcations with nearly identical branch-averaged values may have local deposition profiles that differ by factors greater than 10. This observation highlights the need for local quantitative validations of particle deposition results. However, very few studies consider quantitative validations at the sub-branch level [26]. As a result, it is not clear if current CFD predictions are correctly capturing the localized deposition characteristics of inhaled respiratory aerosols [72, 73]. CFD predictions of local aerosol deposition may be beneficial in predicting absorption, transport, and cellular uptake. However these results should be viewed with caution until further validation is completed with more refined experimental data sets.

1.5 Application of Models to Optimize Respiratory Delivery

As discussed, a variety of models are available for simulating both inhaler and respiratory tract deposition. Both 1-D and 3-D models show reasonable agreement with experiments over relatively broad regions of deposition relative to the scale of the predictions. These models have been applied to better understand the mechanics of aerosol deposition for both ambient and pharmaceutical aerosols. For example, numerical simulations of spray aerosol generation and delivery identified a spray aerosol burst effect which significantly contributes to mouth-throat deposition and could be reduced by extending the aerosol generation time [6]. Based on the current level of model advancement, these simulations are now being applied to improve existing inhaler designs, optimize delivery, develop new delivery modalities, and target the site of deposition in the respiratory tract. In the next section, the development of models for inhalers, the whole-lung, and individual sections of the airways are reviewed. For each region, a specific case study is provided to illustrate how simulations can effectively be applied to improve and optimize respiratory aerosol delivery.

2. Models of Delivery Devices

A number of studies have shown that the type and design of a respiratory inhaler can significantly affect deposition in the respiratory tract. Furthermore, deposition in the inhaler can result in significant aerosol loss and inefficient delivery to the airways. Types of

delivery platforms which are expected to most significantly influence dynamics in the respiratory tract are MDIs and passive DPIs. However, device losses and influence on airflow dynamics are also known to be significant for many next-generation softmist inhalers [55, 57]. Due to the 3-D nature of the flow field, CFD models are typically required to simulate inhaler dynamics, deposition, and the resulting influence of the inhaler on transport in the respiratory tract. Selected studies that have developed models of DPIs and spray inhalers (both MDI and softmist) in the context of device deposition are reviewed below. An application case study is then presented in which a CFD simulation is used to quantify and minimize the depositional loss in a model softmist spray inhaler.

2.1 Simulations of Dry Powder Inhalers

A series of studies by Coates *et al*. [41, 74–76] was first to highlight the advantages of a concurrent CFD and experimental approach for DPI analysis and design. These studies have considered the effects of grid structure and mouthpiece length [76], air inlet size [75], air flow [41], and mouthpiece geometry [74] on powder deagglomeration and deposition for the Aerolizer™ DPI system. Transport characteristics observed with the CFD model were used to explain *in vitro* observations of the performance variables.

Wong et al. [77] recently conducted CFD simulations and experiments in three prototype DPI devices. The deaggregation of particles, which is required for the formation of a small respirable aerosol, was quantitatively linked to both turbulent kinetic energy and particle velocity at the impactor plate. Kroeger et al. [78] described the simulation of dry powder aerosols including particle-to-particle collisions, particle-to-particle detachment, and particle-to-wall interactions. Wong et al. [56] applied CFD modeling in a series of entrance tubes in conjunction with experiments to investigate the influence of turbulence on agglomerate breakup. A critical impaction velocity was identified for effective breakup of the agglomerates. These CFD studies illustrated that most DPIs require wall impaction and turbulent kinetic energy to form a small respirable aerosol. However, these same factors contribute to device deposition and increased aerosol loss in the upper respiratory airways.

2.2 Simulations of Spray Inhalers

Relatively few CFD studies of spray inhalers have been performed. Dunbar et al. [79] developed a CFD model of droplet transport including atomization and evaporation for a MDI system and found good agreement with phase Doppler particle analysis. Versteeg et al. [80] reported a CFD model of MDI transport in an induction port geometry and found primary deposition in the horizontal section, which was consistent with the experimental results of Stein and Gabrio [81]. Kleinstreuer et al. [10] reported a CFD model of MDI aerosol transport and found good agreement with the mouth-throat deposition results of Cheng et al. [82]. Longest et al. [11] developed a CFD model of droplet transport for a capillary aerosol generator and showed good agreement with concurrent *in vitro* deposition results on a sectional basis. Longest et al. [6] then applied this model to analyze the effect of the spray aerosol burst effect on deposition in a mouth-throat geometry. It was found that deposition could be reduced by extending the period of spray aerosol delivery and thereby minimizing the effect of the initial spray burst. Longest et al. [55] reported good agreement between predicted and measured deposition of drug within multiple spray delivery platforms, which included a capillary aerosol generator, MDI, and a Respimat softmist inhaler. Longest and Hindle [57] analyzed the Respimat softmist inhaler and identified significant recirculation within the inhaler mouthpiece which contributes to significant (~30%) deposition of the aerosol in the device. Based on these studies, CFD models appear capable of predicting droplet transport and deposition within and from spray devices; however, their use has not been fully implemented in the design and evaluation of current aerosol delivery systems.

2.3 Application of CFD Modeling to Minimize Aerosol Loss in a Spray Inhaler

Longest and Hindle [42] evaluated the effects of dilution air inlets and flow pathways on mouthpiece drug deposition for a new pharmaceutical spray aerosol inhaler using a concurrent *in vitro* experimental and CFD approach. The spray aerosol system considered was capillary aerosol generation (CAG), which was reported to produce a high fraction of fine (< 5 µm) droplets compared with other liquid-based systems [55]. In previous studies, the transport and deposition of CAG aerosols in induction port and mouth-throat geometries were considered in the absence of an inhaler body and associated coupling mouthpiece [5, 11]. In this study, design aspects of an inhaler body and mouthpiece were evaluated. Ideally, the inhaler was to produce low total mouthpiece drug deposition, or drug loss, and would not significantly alter the reported low values of induction port drug deposition. Two dilution airflow inlet sizes and two flow conditions near the spray nozzle were considered resulting in a total of four prototype inhaler designs. These systems were analyzed using a concurrent *in vitro* and CFD approach. Quantitative correlations were sought that could be used to analyze the four prototypes and could potentially be implemented to optimize future designs. Moreover, this study illustrated the advantages of quantitative analysis and design applied to a model system for a specific set of design variables and a defined performance criterion.

Results of Longest and Hindle [42] indicated that both the size of the upstream dilution air inlets and the flow pathway configuration near the spray nozzle significantly influenced aerosol transport and deposition. CFD results showed that the primary transport characteristics associated with drug deposition were turbulence intensity and the effective diameter of the mouthpiece. Strong quantitative correlations were developed between the identified transport characteristics and mouthpiece drug deposition. For example, Figure 1 illustrates the correlation between mouthpiece deposition fraction (DF) and average turbulent kinetic energy (I_{avg}) resulting in a correlation coefficient R^2 value of 0.997. This design variable can then be applied to minimize mouthpiece deposition of the spray aerosol, illustrating the utility of the simulation results in device development and optimization for respiratory aerosol delivery.

3. One-Dimensional Whole-Lung Aerosol Deposition Models

Traditional whole-lung deposition models can be classified as semi-empirical, single path, or stochastic. The categories of single path and stochastic refer to how the lung geometry is approximated in the model. With both of these model types, the correlations that account for deposition by various mechanisms may be semi-empirical, analytical, or stochastic. Traditional whole-lung models were previously reviewed by Finlay [83], Martonen et al. [39], and Martonen et al. [84]. Isaacs et al. [14] reviewed mechanisms of aerosol deposition in the airways. However, traditional whole-lung models are discussed below for completeness followed by recent advances that make these models more applicable to pharmaceutical aerosols and drug delivery.

3.1 Traditional Whole-Lung Models

Traditional semi-empirical models provide correlations for whole-lung deposition or regional deposition based on fitting empirical data as a function of analytical parameters. For larger aerosols around 1 µm and above, an impaction parameter or the more physically relevant non-dimensional Stokes number is used. To capture diffusional deposition, a non-dimensional diffusion parameter is often employed [85]. The study of Stahlhofen et al. [15] summarized previous *in vivo* deposition data and presented correlations for upper airway (fast clearance) and lower airway (slow clearance) deposition fractions based on impaction and diffusion parameters. The study of Rudolf et al. [86] presents similar correlations with the inclusion of tidal volumes to better account for the effects of inter- and intra-subject

variability on the deposition results. The studies of Kim and Jaques [87] and Kim and Hu [88] present similar total lung deposition correlations. Based on the underlying data, these correlations are appropriate for monodisperse stable (constant diameter) spherical aerosols inhaled under controlled conditions through a large mouthpiece.

In contrast with whole-lung semi-empirical correlations, single path models were the first to predict branch-averaged deposition throughout the respiratory tract. These models assume all branches at each level of the tracheobronchial tree have equal dimensions, such that the aerosol passes down an average single path of the lung. Within each branch, deposition is calculated as a function of individual mechanisms, which typically include sedimentation, impaction, and diffusion. Typical single path models were developed and presented in the studies of Taulbee and Yu [51], Yeh and Schum [49], Martonen [89], Martonen [4], ICRP [1, 2], and NCRP [3]. As described by Martonen et al. [39], these single path models can account for factors such as intersubject variations in lung geometry, ventilatory parameters, and complex aerosol physics. Overall, these models agree well with *in vitro* fast and slow clearance fractions, which are assumed to represent upper and lower airway deposition, respectively [39, 83]. However, agreement with *in vivo* data is typically of lowest quality for aerosols greater than 5 µm and for all sizes in the alveolar region. In addition to healthy adults, single path models have also been used to explore aerosol deposition in approximations of diseased lungs [90, 91] and pediatric airways [92, 93].

Stochastic whole-lung models attempt to capture both the probability for deposition and the expected variability in deposition on a branch-averaged basis. The first of these models was developed by Koblinger and Hofmann [94, 95] and used a Monte Carlo simulation to generate a random path from the mouth through the alveolar sacs. Deposition within each airway structure was calculated based on traditional correlations for sedimentation, impaction, and diffusion. The process of generating a random pathway and calculating deposition was repeated for a sufficient number of randomly generated structures to allow for the calculation of statistical mean values of deposition with standard deviations at each branch level. Asymmetry of the airway bifurcations and flow was included in the model. The study of Hofmann and Koblinger [96] showed good agreement of the Monte Carlo 1-D lung model with fast and slow clearance deposition fractions from *in vivo* studies. Asgharian et al. [21] described the use of the Monte Carlo lung geometry approach in the development of the MPPD model. Applications of this approach include an assessment of intersubject variability in particle deposition throughout the respiratory tract [97] and the deposition of nanoaerosols [98]. The effects of asymmetrical lung ventilation on lobar deposition have also been explored using this modeling platform [99, 100].

Predictions of traditional 1-D models for upper and lower airway deposition usually fall within the wide range of experimental results, which arises due to intersubject variability in the experiments. Expanding *in vivo* data is helping to better identify expected means of deposition as a function of patient age [101] and gender [88]. The bolus delivery technique of Kim [102] allows for the determination of deposition through a series of inhalation volumes. Comparisons can then be made with 1-D model results throughout regions of the airways. However, experimental data for validating model predictions at the branch-averaged level remains elusive. Current imaging techniques have reported branch-level deposition data through the sixth respiratory generation [103]. For more distal airways, significant assumptions are required related to the mapping of airways into a 3-D shell model of the lung [39]. Using an advanced mapping model, Fleming et al. [104] compared *in vivo* deposition with predictions of the ICRP model on a branch-averaged basis. While some aspects of the predictions matched the *in vivo* results, there were significant differences in central vs. peripheral deposition and in the amount of alveolar deposition vs.

the amount exhaled. Advances in imaging techniques and expanded data sets are needed for more convincing validations of 1-D model predictions at the branch-averaged level.

3.2 Advancements for the Simulation of Pharmaceutical Aerosols

A number of recent advances have made whole-lung models more capable of determining the deposition of pharmaceutical aerosols. The study of Martin and Finlay [105] proposed a whole-lung deposition correlation based on most all available *in vivo* data. The correlation accounts for inhalation flow rate, tidal volume, patient functional residual capacity as well as particle and gas variables. Kim [102] summarized whole-lung deposition correlations based on the studies of Kim and Jaques [87] and Kim and Hu [88].

Pharmaceutical aerosols are expected to vary in size as a function of either evaporation or hygroscopic growth. Ferron [106] developed a general model for hygroscopic aerosol growth in the respiratory airways, which was applied to pharmaceutical aerosols in the study of Ferron et al. [18]. At typical respiratory tract conditions, which are generally considered to be 99.5% relative humidity and 37 °C, Ferron et al. [18] showed that the effect of hygroscopic growth on aerosol size increase was significant for many common drugs and salts at dilute aerosol number concentrations. Similar results are expected from the study of Martonen [89]. For nebulized droplets, the study of Finlay and Stapleton [107] showed that aerosol number concentration greatly reduced the potential for evaporation due to saturation of the continuous phase. Finlay [108] developed a generalized theory on droplet hygroscopic growth and evaporation and found that little size change is expected for nebulized droplets at number concentrations typical of pharmaceutical aerosols. Other recent whole-lung studies that consider droplet size change include Broday and Georgopoulous [17] and Varghese and Gangamma [109].

An area where whole-lung modeling has been significantly improved is in the prediction of alveolar deposition. In the alveolar region, deposition typically occurs due to sedimentation and diffusion. Both of these mechanisms are strongly influenced by wall motion, which is known to be significant in the flexible alveolar airways during respiration. A representative study that accounts for the effects of alveolar wall motion was performed by Choi and Kim [110]. In this model, alveolar transport was treated as a two dimensional process by accounting for both radial diffusion and alveolar motion during airway expansion and contraction. Kim [102] reports notable improvements of model predictions in comparison with experimental results.

Other advances in whole-lung models include the consideration of non-spherical particles or drug delivery fibers [111], the effects of particle charge [19], and bolus dispersion. Both MDI and DPI aerosols are delivered as a bolus to the airways. Traditional deposition models often neglect factors associated with bolus delivery, which may influence the local deposition pattern within the airways. The study of Park and Wexler [112] presented a bolus dispersion model based on differences in inhalation and expected exhalation velocity profiles. Park and Wexler [113] illustrated the motion of particles in the smaller range of the pharmaceutical aerosol spectrum over multiple breaths within the lung, which can affect both the site and amount of deposition.

3.3 Application of Whole-Lung Models to Develop Charge-Targeted Delivery

Over 50 years ago, Wilson [114] suggested the potential for enhanced aerosol deposition in the respiratory tract due to particle charge. Currently, charge on pharmaceutical aerosols is thought to affect deposition in sizing devices [115], inhalers [116], and the respiratory tract [19]. Studies by Yu [117], Thiagarajan and Yu [118], and Chen and Yu [119] developed analytical expressions for charged particle deposition in geometric elements consistent with

sections of the respiratory tract. The subsequent studies of Balachandran et al. [120] and Bailey et al. [121] used 1-D whole-lung models to describe targeting the deposition of pharmaceutical aerosols to specific lung regions by controlling the inhalation flow rate, particle size, and level of charge. Balachandran et al. [120] showed that charge effects could be more significant than sedimentation in the alveolar airways and could target deposition to this lung region. Bailey et al. [121] observed that charged submicrometer particles significantly increased alveolar deposition whereas charged micrometer particles were largely retained in the upper airways. Currently, a practical system for delivering a charge-targeted pharmaceutical aerosol has not been developed. This is largely due to difficulties in generating consistently charged aerosols without significant depositional losses. The most practical way to effectively generate a charged aerosol for inhalation may be electrospray [122]. However, this method of aerosol generation requires high voltages in the inhaler and likely generates a small amount of ozone, which can irritate and inflame the respiratory tract. Finlay [83] suggested that the humid environment of the respiratory tract will diminish particle charge, which is expected to reduce the effectiveness of charge targeting. While current technological limitations may prohibit the practical delivery of charge-targeted aerosols, the modeling studies of Balachandran et al. [120] and Bailey et al. [121] illustrate the use of a numerical whole-lung model to develop a potential respiratory aerosol delivery system capable of providing targeted delivery to the upper or lower respiratory tract that may prove useful in future applications.

4. CFD Models of Aerosol Deposition in the Extrathoracic Airways

An understanding of deposition in the extrathoracic airways is critical because aerosols depositing in this region are not available for delivery to the remainder of the respiratory tract. Extrathoracic deposition is usually high for both ambient and pharmaceutical micrometer aerosols. Furthermore, significant variability in extrathoracic airway geometries coupled with high depositional losses creates high variability in the aerosol dose delivered to the lungs [123]. CFD models have frequently been applied to better understand the deposition of both ambient and pharmaceutical aerosols in this region. As reviewed below, these models are currently being applied to develop devices that reduce extrathoracic deposition, and the associated variability, in the case of lung delivery or to target deposition within specific regions of the nose for nasally administered drugs.

4.1 Deposition in Mouth-Throat Models

Considering stable orally inhaled ambient aerosols, CFD studies have been used to evaluate transport and deposition in simplified, patient specific, and characteristic mouth-throat (MT) geometries. The MT region is typically considered to contain the oral cavity, pharynx, larynx, and sometimes an upper portion of the trachea. In general, simplified models have a geometric similarity to the airway region being considered, but may leave out key details that affect the output variables of interest. Patient specific models are based on reconstructions from medical images of individual subjects, and attempt to include all geometric details available in the scans. In contrast, characteristic models seek to accurately reproduce the aerosol deposition characteristics of a specific patient population while omitting unnecessary geometric details that do not affect the variables of interest. Kleinstreuer and Zhang [124] developed a simplified model of the MT that was characterized by a curved airway and circular cross-sections based on the hydraulic diameters specified by Cheng et al. [125]. This study showed good agreement between the regionally averaged empirical data of Cheng et al. [125] as a function of Stokes number and the numerical results. Kleinstreuer and Zhang [124] also demonstrated the importance of transitional and turbulent flows on particle deposition throughout the oral airway model. Zhang and Kleinstreuer [126] used this oral airway model to characterize local species heat

and mass transfer. Zhang et al. [33] mapped localized deposition values for a range of flow rates and particle sizes in the same circular oral airway model.

Patient specific models of the MT region have been developed to consider a variety of aspects related to the deposition of ambient aerosols using CFD modeling. Sosnowski et al. [127, 128] applied a patient specific model of the MT to characterize the effects of non-steady flow on the deposition of aerosols in the size range of 0.3 – 10 µm. This study highlighted the potential importance of aerosol or bolus release time on deposition in the extrathoracic airways. Takano et al. [129] developed a patient specific MT model with a focus on realism in the laryngeal region. This study indicated that a majority of deposition occurs in the oral cavity and pharynx with deposition in the larynx agreeing with ICRP [1] model predictions. Jayaraju et al. [130] developed a similar patient specific model of the oral cavity using an unstructured grid and also found that a majority of deposition occurred in the oral cavity. Studies by Gemci et al. [131] and Sandeau et al. [132] have considered patient specific models of the larynx and MT, respectively, and demonstrated reductions in aerosol depositional losses for administration with low density helium-oxygen mixtures, which act to effectively reduce inertial impaction and turbulence.

The study of Stapleton et al. [133] was the first to report a characteristic MT model which was based on simple geometries and retained basic anatomical features from medical scans as well as direct observations of living subjects. This model is referred to as the Alberta MT geometry, and has been widely implemented in both numerical and *in vitro* aerosol deposition studies [52, 134–137]. Using this MT model, Stapleton et al. [133] reported good agreement between CFD model predictions and *in vitro* experimental results of total aerosol deposition for laminar flow but not for turbulent conditions using a k-ε turbulence approximation. Matida et al. [52] reported that poor agreement between model and experimental results using Reynolds averaged Navier Stokes (RANS) approaches like the k-ε model was due to the assumption of isotropic near-wall turbulence, which assumes turbulent fluctuations are equal in all directions [23]. Significant improvements in model agreement with experimental data were achieved with the use of a near-wall anisotropic correction to the RANS model. Zhang et al. [137] developed a further simplified characteristic geometry of the MT and evaluated the geometry using both CFD simulations and experiments. The CFD model results, using a k-ω model and near-wall corrections, agreed with deposition experiments and showed that this highly idealized geometry may be a good characteristic model of MT deposition. Zhang et al. [138] used CFD modeling and experiments to optimize the highly idealized MT to best match the deposition profiles of *in vivo* data.

Xi and Longest [31] used a CFD modeling approach to develop a characteristic MT geometry based on successive geometric simplifications of a realistic geometry. It was found that a MT model composed of smoothly connected elliptical cross-sectional profiles provided good agreement with deposition in the realistic geometry for both micrometer [31] and nanometer [139] aerosols. This model has also shown good agreement with patient specific *in vitro* [140] and *in vivo* data [15], as reported by Longest et al. [5]. Xi and Longest [31] reported that the inclusion of a non-circular glottic aperture was required to accurately model deposition in the region of the larynx. Furthermore, the use of an elliptical glottis and sloped trachea in the elliptical model of Xi and Longest are expected to provide realistic inlet conditions for considering deposition in models of the tracheobronchial airways, as reported by Xi and Longest [31] and Xi et al. [45].

Considering pharmaceutical aerosol transport in the respiratory airways, several CFD studies have evaluated the effects of DPI inlet conditions on enhanced aerosol deposition. Matida et al. [141] considered transport in the MT region with different small size tubular inlets using

CFD modeling and confirmed that a turbulent impinging jet striking the back of the throat was responsible for an experimentally observed [136] inverse relationship between inlet size and MT deposition. With insights gained from this modeling study, DeHaan and Finlay [7] developed a novel quantitative correlation to predict oral cavity deposition as a function of Stokes number and mouthpiece diameter. This correlation can be used to optimize the geometry of DPI mouthpieces in order to minimize oral cavity losses for specific aerosol sizes. Matida et al. [12] considered transport in an oral cavity model with a 3 mm inlet consistent with a typical DPI using large eddy simulation (LES) turbulence modeling. Both turbulence and the inlet jet were shown to significantly elevate MT deposition. Furthermore, LES was shown to provide better agreement with experimental results than an isotropic RANS approach (i.e., without near-wall anisotropic corrections). Ilie et al. [61] evaluated aerosol transport and deposition in the oral airway for a small DPI inlet with a spiral design. Large eddy simulations were shown to match experimental deposition results very well. However, Ilie et al. [61] stress the high computational cost of LES, which makes this method impractical for simulating transient inhalation profiles.

Due to the complexity of the underlying physics, the transport and deposition of pharmaceutical spray inhalers have only recently been successfully modeled. Kleinstreuer et al. [10] evaluated chlorofluorocarbon (CFC) and hydrofluoroalkane-134a (HFA) MDIs connected to a MT model. The CFD simulations started with a large size aerosol at the actuator nozzle and modeled secondary droplet breakup, evaporation, two-way momentum coupling, and heat/mass transfer. The CFD model predictions matched previously reported values of aerosol drug deposition in the MT region. The study of Kleinstreuer et al. [10] also described the delivery of spray aerosols within pre-determined locations of the mouthpiece inlet to target deposition within the airways. Longest et al. [55] considered an MDI inhaler connected to an induction port model. In this study, *in vitro* experiments were first used to determine the initial distribution of the polydisperse pharmaceutical aerosol. The flow field simulation included an evaluation of compressible and supersonic flow as the propellant exited the 250 µm actuator orifice. Simulation predictions match concurrent *in vitro* experiments of drug deposition in the inhaler mouthpiece and induction port.

Longest and Hindle have considered the aerosol dynamics of a series of next-generation softmist inhalers connected to MT models using a concurrent CFD and *in vitro* approach. Longest et al. [11] developed a CFD model of CAG in which an aerosol is formed by pumping a liquid through a heated microcapillary. Results of the CAG model showed excellent agreement with *in vitro* deposition experiments in a sectioned induction port geometry. The study of Longest et al. [5] evaluated the effects of spray momentum on drug deposition in induction port and MT geometries compared with ambient aerosols. Spray momentum was shown to increase the mouthpiece and MT deposition of pharmaceutical aerosols through the mechanisms of (1) induced turbulence and (2) significant droplet inertia. To reduce spray momentum, Longest et al. [6] used CFD simulations to explore the effects of extending the aerosol generation time. Longest and Hindle [57] used concurrent CFD modeling to evaluate spray transport from the Respimat inhaler and to describe mechanisms responsible for high inhaler deposition, as described previously in this review. Size change was observed to be significant for MDI aerosols, but two-way coupling and the effect of spray momentum generally limited the effects of evaporation for the other spray systems considered.

4.2 Nasal Deposition

Previous CFD studies of aerosol transport and deposition in the nasal airways have considered aerosols in the ultrafine (<100 nm), fine (100 nm – 1 µm), and coarse (>1 µm) regimes. Comparisons of CFD results to experimental deposition data for submicrometer aerosols in the nasal airways are often difficult due to differences in the geometric models

and the complexity of the transport dynamics. Martonen et al. [142] developed a numerical model of ultrafine aerosol transport and deposition in the nasal cavity based on diffusional theory in a highly simplified tubular geometry. The resulting correlation agreed well with experimental predictions of total deposition for nanoparticles ranging from 1 – 100 nm. More recently, Shi et al. [143] reported local deposition patterns of very small nanoparticles in the nasal cavity under laminar and transient breathing conditions based on a chemical species transport model. Zamankhan et al. [144] simulated the transport and deposition of ultrafine aerosols in the range of 1 – 100 nm and showed good agreement with the *in vivo* deposition data of Cheng et al. [145] for particles less than approximately 20 nm. However, particles greater than 20 nm did not match the experimental data to a high degree.

Considering both fine and ultrafine aerosols, Xi and Longest [27] presented a novel drift flux model to effectively simulate the transport of aerosols less than 1000 nm, which is often numerically challenging due to the small amount of inertia that must be accurately resolved [73]. The drift flux method matched existing *in vitro* and *in vivo* nasal deposition data to a high degree.

For coarse aerosols, Schroeter et al. [146] considered the effect of size, nostril release position, and flow rate on local deposition in the nasal airways. These results can be used to select optimal conditions for respiratory drug delivery to specific regions of the nose. However, initial spray momentum and droplet velocity were not present in the simulations. Liu et al. [60] simulated particles ranging from 0.354 – 16 µm using three Lagrangian particle tracking models. Results of this study showed that the standard eddy interaction model used for Lagrangian particle tracking in turbulent flows significantly over predicted the deposition of the smaller particles considered. Shi et al. [147] developed a model of wall roughness to improve the agreement between numerical simulations and nasal cast experiments. Shanley et al. [148] conducted CFD simulations for nasal aerosols in the size range of 1 to 10 µm and provided an improved correlation for deposition. Schroeter et al. [149] recently showed that both surface roughness and model smoothness must be considered to successfully match *in vitro* results for inertial particle deposition.

Compared with ambient particles, pharmaceutical aerosol delivery in the nasal airways has been considered by significantly fewer studies. Schroeter et al. [150] considered the hygroscopic growth of cigarette smoke (which is not a pharmaceutical aerosol) in the nasal airways and reported significant changes in droplet size. Kimbell et al. [151] considered CFD simulations of aerosol transport from spray devices, as described below. Longest et al. [152] used CFD simulations to explore the delivery of pharmaceutical aerosol through the nose and into the lungs using the concept of enhanced condensational growth.

4.3 Application of CFD Modeling to Target Nasal Delivery

Aerosol deposition in the nasal airways can be used to effectively administer both systemic and locally acting pharmaceuticals. For optimal absorption and uptake, deposition is required beyond the nasal value region. However, studies typically indicate that nasal sprays are deposited within the anterior 1/3 of the nose (i.e., the vestibule and valve regions). The experimental study of Foo et al. [153] recently showed that nasal spray deposition is largely controlled by spray properties, such as spray cone angle and initial velocity. However, few CFD studies have included spray properties in the simulation of nasal deposition. To optimize the nasal delivery of sprays for aerosol deposition beyond the valve region, Kimbell et al. [151] considered aerosol transport and deposition in a patient specific nasal model. CFD simulations were used to evaluate the effects of spray properties (inhaler angle and initial droplet velocity), nozzle insertion depth, particle size, and inhalation flow rate on deposition beyond the nasal value. For optimal conditions, post nasal valve deposition was observed to increase by an order of magnitude from typical values of approximately 2% to

values of 20%. Moreover, release positions within the nostrils were mapped that can be used to further optimize post nasal valve delivery and control the site of deposition. The effective targeting of sprays to specific regions of the nose, like the olfactory region for nose-to-brain delivery, is an area in which CFD simulations can make future contributions.

5 CFD Models of Tracheobronchial Deposition

A number of studies have used CFD simulations to predict aerosol deposition in simplified, patient specific, and characteristic models of the upper conducting airways. Simulating deposition in the tracheobronchial (TB) region has recently been reviewed by Kleinstreuer et al. [64]. Specific areas of interest for ambient aerosols that contribute to the simulation of pharmaceutical delivery include validations of simulation results, evaluation of localized deposition, CFD model selection, and development of composite CFD models of the entire TB airways. For pharmaceutical aerosols, studies have focused on droplet growth and evaporation with dissolved solutes. These topics are reviewed below and a case study is presented in which a new respiratory aerosol delivery approach is developed using CFD simulations in conjunction with concurrent *in vitro* testing.

5.1 Simulations of Ambient Aerosols in the TB Airways

Simulations of ambient aerosol deposition in the TB airways have been compared with experimental results in a number of studies. In simplified double bifurcation models, branch-averaged deposition has been widely compared with the *in vitro* data of Kim and Fisher [154] [32, 67, 68, 155, 156]. Considering localized conditions, Longest and Vinchurkar [157] compared deposition results for a 10 µm aerosol using a LRN k-ω model with the mm-scale *in vitro* data of Oldham et al. [158]. It was determined that correctly modeling the inlet velocity and particle profiles was required to accurately reproduce the localized deposition results. Furthermore, agreement between the model and experiments in terms of total deposition did not indicate validation of the model on the local level. Difficulties with validating CFD deposition results were further explored in Longest and Oldham [159] and Oldham [160]. In a more complex geometry of the lower TB airways, Robinson et al. [161] calculated the deposition of submicrometer particles and validated the total deposition values with *in vitro* experiments in the same model. Isaacs et al. [54] considered a simple model of the trachea and successfully compared with previously published results of local particle deposition at the first carinal ridge. Using an accurate scan based representation of an existing TB cast geometry through the sixth generation, Xi and Longest [45] successfully predicted total *in vitro* deposition results over a range of particle sizes from Cohen et al. [162] and Gurman et al. [163] in the same model (Figure 2). Recent studies by Tian et al. [35] and Lambert et al. [30] have successfully compared with *in vitro* TB deposition results on a branch averaged level. However, detailed validations of local particle deposition and hotspot formation in the TB airways remains to be performed.

CFD simulations provide the capability to map localized regions of deposition, which are frequently referred to as hot spots. Quantifying the amount of deposition within hot spots is important to accurately predict particle dissolution in mucus or airway surface liquid, diffusional transport after deposition, and uptake within the epithelial layer. Balashazy et al. [34] describe the calculation of hot spots and Balashazy et al. [66] associate hot spot formation with the occurrence of tumors in lung cancer, which was also shown by Martonen [164] using an *in vitro* model. A number of studies in simplified geometries have presented deposition enhancement factors (DEFs), which quantify the amount of local deposition within a defined area relative to total deposition in the entire region considered. For a simplified upper TB model, Zhang et al. [33] showed that DEFs for microparticles ranged from 40 to 2400 and for nanoparticles ranged from 2 to 11. Longest et al. [32] indicated that 30% asthma constriction of upper airway diameters could increase DEFs in the upper TB

airways by one to two orders of magnitude; a new microdosimetry factor was also defined for calculating doses within hot spot regions. For a CFD model of the TB airways based on an airway cast (see Figure 2 insert), DEFs computed by Xi and Longest [45] are presented in Figure 3.

In calculating CFD simulations of aerosol deposition, modelers can choose between several meshing options. Longest and Vinchurkar [72] illustrated that commonly used and easy to construct tetrahedral meshes reduce solution quality and increase simulation times. In contrast, hexahedral mesh designs require more initial time and expertise to generate, but provide faster solutions and a better match to *in vitro* experimental data. Vinchurkar and Longest [165] showed that for 10 µm particles, there was little effect of the mesh on local deposition patterns. However, both local and total deposition fractions changed dramatically for smaller particles as a function of mesh type with the hexahedral mesh providing the best results.

As with the extrathoracic airways, the selection of the turbulence model in the TB region can significantly affect the quality of the deposition results. The study by Jayaraju et al. [166] considered an idealized upper airway model that contained a portion of the trachea and showed that detached eddy and large eddy simulations improved agreement with experimental results for the prediction of the flow field and micrometer particle deposition, compared with a RANS k-ω turbulence model without near-wall corrections. However, studies by Longest and Vinchurkar [157] and Xi et al. [45] indicated that the LRN model can accurately predict local and total particle deposition, provided that a near-wall correction is included. Longest and Xi [25] also showed that corrections to the Brownian motion term and improved interpolations of near-wall velocities were required for the accurate simulation of nanoaerosols using a common commercial code (i.e., Fluent 6.2/6.3/12, ANSYS Inc., Canonsburg, PA). Studies by Jin et al. [62] and Lambert et al. [30] have considered LES in the upper TB region for ambient particle deposition. However, simulating transient inhalation waveforms remains computationally prohibitive for LES. Studies by Zhang et al. [70] and Li et al. [167] have indicated that the inhalation waveform may affect the deposition of aerosols in the upper TB airways.

In addition to multiple options for turbulence modeling and selecting steady state or transient airflow conditions, different types of particle tracking models are also available and have been applied in the TB airways. Particles can be simulated as either discrete elements (Lagrangian model) or as a second continuous phase (Eulerian model). A recently developed Eulerian model of ambient aerosol transport and deposition in the TB airways shows excellent agreement with total and local *in vitro* results [26], can decrease particle simulation times by an order of magnitude [28], and is not subject to over predictions of deposition associated with isotropic turbulence models.

A number of recent papers have reported aerosol transport and deposition in realistic models of the upper TB airways usually extending to approximately the fourth through the ninth generations for inhaled ambient aerosols [45, 167, 168]. Gemci et al. [169] developed a CFD model of airflow in all generations (~17) of the TB region. However, the reported number of grid cells was likely not sufficient when compared to the grid convergence studies of Longest and Vinchurkar [72]. In a series of papers, Kleinstreuer *et al*. developed a CFD model of aerosol transport and deposition throughout the TB region [36, 170]. This model is based on repeating scaled triple bifurcation units in series and in parallel to characterize airflow and deposition in all 16 generations of an idealized TB tree, and is effective for evaluating deposition efficiency within individual branches. Lin et al. [37] reported a coupled 3-D and 1-D lung transport model that can mimic the entire TB region on a patient specific basis; however, particle transport results were not provided. Lambert et al. [30]

developed a patient specific model of steady state inhalation using LES that extended from the mouth to approximately the sixth respiratory generation. This CFD study was then used to explain the disproportionate fraction of aerosols that is known to enter the left lung despite higher ventilation to the right lung.

5.2 Models of Pharmaceutical Aerosols in the TB Airways

Compared with ambient particles, significantly fewer studies have considered the transport and deposition of pharmaceutical aerosols in the TB airways. While not a pharmaceutical aerosol, the unexpected high deposition of cigarette smoke in the upper TB airways was considered using a CFD model of hygroscopic droplet growth by Longest and Xi [171]. Using salt as a model pharmaceutical solute, Zhang et al. [172] showed that concentrations of 10% and higher were required for hygroscopic growth to have a significant impact on deposition.

Both computational and *in vitro* studies have been used to develop the recently proposed concept of enhanced condensational growth (ECG) aerosol delivery [8, 173]. In this approach, a submicrometer- or nanometer-scale aerosol is delivered to the respiratory airways in conjunction with an airstream that is saturated or supersaturated with water vapor and above body temperature. Aerosols in the size range of 100 – 1000 nm are considered in order to minimize deposition in the extrathoracic airways and maximize the dose of delivered drug. As a result, aerosol depositional loss in the delivery device and MT or nasal region are largely eliminated. The inhaled water vapor is used to create supersaturated conditions within the respiratory airways. Submicrometer droplets in this supersaturated environment increase in size at a controlled rate due to condensation. Size increase to within the range of 2 – 3 µm is used to ensure deposition and full lung retention of the aerosol.

Hindle and Longest [43] evaluated ECG aerosol delivery in a characteristic model of the MT and upper TB region extending to the fifth respiratory bifurcation (B5) down an individual path using concurrent CFD simulations and experiments. Results indicated that MT drug loss was minimal (~1%) and that TB deposition increased with ECG conditions, which implies significant aerosol growth. Specifically, ECG conditions were observed to increase deposition in branches B3 – B5 by an order of magnitude compared to a control case without growth (~2% with ECG vs. 0.3% with control). The numerical predictions closely matched the experimental results of deposited drug within individual sections of the model and indicated a size increase of the initially submicrometer aerosol to 2 – 4 µm at the fifth respiratory bifurcation. As a result of this and previous concurrent CFD and *in vitro* studies, it can be concluded that ECG is an effective strategy for significantly reducing MT aerosol deposition and increasing droplet size to a target range of 2 – 4 µm, which is expected to produce nearly complete lung retention.

5.3 Application of CFD Modeling to Evaluate the Performance of ECG Delivery

Tian and Longest [35] recently used CFD simulations in a characteristic MT and TB model to further develop the concept of ECG delivery. In this study, ECG delivery was evaluated in an individual path model extending from the MT to the end of the TB region. Initially monodisperse aerosol sizes of 560 and 900 nm were delivered at the mouth, consistent with previous experimental studies [173]. Aerosol size change and deposition were assessed for the inhalation of control subsaturated air and ECG conditions with saturated air and temperatures of 39 and 42 °C. Results indicated that both the control and ECG delivery cases produced very little deposition in the MT and upper TB model (approximately 1%). Under ECG delivery conditions, large size increases of the aerosol droplets were observed resulting in mass median aerodynamic diameters of 2.4 – 3.3 µm exiting the fifth branch of the TB airways (Figure 4a). This increase in aerosol size produced an order of magnitude

increase in aerosol deposition within the TB airways compared with the controls, with TB deposition efficiencies of approximately 32 to 46% for ECG conditions (Figure 4b) based on the CFD model. Estimates of downstream pulmonary deposition indicated near full lung retention of the aerosol during ECG delivery.

6. CFD Models of Aerosol Deposition in the Alveolar Airways

There are a number of analytic benchmark models of the acinar region dating back more than 50 years, but it has not been until recently that CFD models have contributed to the understanding of transport and deposition in the alveolar airways. Studies of deposition have progressed from analytic 1-D models of the whole lung to 3-D numerical models that expand and contract rhythmically [65] while providing extremely accurate geometric details for multiple generations [174]. This region has always been difficult to consider experimentally because the particles that reach the alveolar region are capable of depositing by four modes - inertia, sedimentation, diffusion and wall induced convection, and a model that describes deposition must account for each of these mechanisms. This stands in contrast to models of oxygen and carbon dioxide molecular transport, which move primarily by diffusion. Berg *et al*. [175] show the level of geometric complexity required to create an *in vitro* physiologically accurate model of the alveolar airways. Using modeling, Kojic and Tsuda [176], Haber [177], and Schirrmann *et al*. [178] demonstrate the importance of flow conditions and cyclic breathing in the alveolar airways.

6.1 Transport and Deposition in a Single Alveolus

Modeling the alveolar airways as a single alveolus provides a baseline for understanding the mechanics which govern the transport and deposition of particles in the deep lung. Particle size, wall motion, breathing cycle, and orientation of gravity have all been shown to significantly affect deposition. Kojic & Tsuda [176] used an analytic model to solve non-dimensionalized particle motion and deposition equations and determined the importance of oscillatory flow conditions. The application of the classical assumption of steady Poiseuille flow to an alveolus significantly underestimated local deposition density.

In early alveolar models, inertia was not typically considered because of the "creeping" flow of air and corresponding low Reynolds number (Re << 1) [179]. Similarly, convective mixing was traditionally excluded from the model because of the low Reynolds number. Further simplifying the early models, the motion of the walls was considered reversible [180] and excluded. These simplifications lead to highly predictable streamlines and deposition that was not realistic [181]. Haber *et al*. [177] built analytical and numerical models to demonstrate the complexity of streamlines in a single alveolus. Their findings indicate convective mixing in the alveolar region stemming from the interaction of the wall motion and the breathing cycle even though the Reynolds number was very low. As a result, models of a single alveolus have shown the importance of including wall motion and convective mixing.

Haber *et al*. [179] describe the complexity of gravitational deposition and deposition of fine particles (diameter < 0.5 µm) in their CFD model of a single alveolus with rhythmically expanding and contracting walls and transient flow characteristics. This study states "…the rhythmical motion of the alveolar walls, fundamentally changes the acinar flow patterns and substantially alters the fate of particles moving inside the alveoli." A transition between sedimentation and diffusion driven deposition appears to occur in the acinar region of the lungs for particles of size ~ 0.5 µm. Balashazy *et al*. [182] built a 3-D expanding and contracting CFD model to determine a transitional range to be 0.1 µm and 1 µm, the largest particles being dominated by sedimentation and the smallest depositing by Brownian

motion. Darquenne & Paiva [183] used a CFD model to estimate this critical particle size to be 0.5 µm, with consistent explanations for the deposition of larger and smaller particles.

6.2 Transport and Deposition in Alveolar Structures

Alveolar structures are groupings or clusters of individual alveoli, which prove more difficult to resolve using analytic models. As a result, 3-D CFD models have been used to explore aerosol transport and deposition in these structures. Lee and Lee [184] numerically compared a rigid cylinder to an expanding cylinder and a rigid alveolated duct to a rhythmically expanding and contracting alveolated duct. Their models found the Strouhal number to be the dominant parameter for particle dispersion and the fluid flow patterns were observed to change between the rigid and expanding geometry, resulting from fluid being pushed or pulled from the alveoli to the central duct. Similarly, Tsuda *et al.* [185] reported complex chaotic flow behavior as the classical assumption of Poiseuille flow was shown to be invalid for a model which considered time-dependent wall motion of a simplified alveolar structure.

Darquenne and Paiva [183] modeled transient breathing in 2-D and 3-D representations of the last four generations and demonstrated that "1D simulations underestimate the penetration of the aerosols in the structure and overestimate the deposition." Dailey and Ghadiali [186] numerically solved for the flow field in a 2-D model of a cluster of alveoli coupled with the motion of the wall. They concluded that particles smaller than 0.5 µm deposit due to the dominance of Brownian diffusion, particles which are larger than 1 µm deposit primarily due to gravitational settling, and particles that are larger than 0.5 µm and smaller than 1.0 µm experience a large residence time due to the diminished diffusion and sedimentation terms.

With a 14 sided representation of an alveolus, Sznitman et al. [65] numerically explored a 3-D model of 8 generations of the pulmonary acinar tree with transient breathing and moving walls and showed that there is a significant loss of kinematic information when models are simplified to a single alveolus or duct. They found 1 µm particles to exhibit highly three dimensional motion due to the residence time being longer than a breathing cycle, which was caused primarily by the oscillatory breathing and suggests that it may be necessary to simulate more than a single breathing cycle.

6.3 Application of CFD Modeling to Evaluate the Delivery of Magnetic Aerosols

Xie et al. [187] evaluated the deposition of aggregated superparamagnetic nanoparticles by conducting kinematic studies in a rigid tube with steady flow using *in vitro* experiments and CFD modeling. This study varied the particle size, tube diameter, and flow rate in the *in vitro* and *in silico* models, but they only considered one orientation of gravity (against flow). Both magnetic effects and Brownian diffusion were considered in the CFD model. Excellent agreement between experimental and numerical simulations was found, with primary differences attributed to the diffusing of the magnetic field at the boundaries and rolling of the particles after contacting the wall. This study provides a baseline for future work in more realistic geometries at various orientations to examine the relationship of magnetic particle deposition in the context of the previously discussed complexities of the acinar region.

In a following study, Xie et al. [188] compared CFD, experimental, and *in vivo* models to characterize the deposition of a polydisperse aerosol with magnetite particles coated in oleic acid. They found no increased deposition in the mouse trachea, due to the distance between the trachea and the magnetic source. However, they showed an increase (doubling) of deposition throughout the airways. Deposition *in vitro* and *in silico* was used to predict deposition *in vivo* by comparing the magnetic deposition time with the aerodynamic time. If

the time required for deposition due to the magnetic force was less than the time spent in the geometry, as determined by the computational model, deposition occurred. Applying this to the acinar airways, the aerodynamic time of the alveolar region is taken to be the amount of time the particle can be found in the deep lung. For complete deposition in the alveolar region, the time found can be determined by dividing the average alveoli diameter by the induced magnetic velocity. Magnetic particles that reach the alveolar region and are retained for two seconds require an induced magnetic velocity of 0.15 cm/s for full deposition. Magnetic velocities predicted by the CFD model showed that pulmonary targeting is possible, and Xie et al. [188] state "This approach can form the basis for assessing the feasibility of magnetic targeted drug delivery in humans." However, when designing future models, the need for a strong magnetic field to induce deposition at large distances must be considered. To address this issue, studies by Martin and Finlay [189] and Redman et al. [190] have proposed using magnetic alignment of fibers to target drug deposition; however, a CFD optimization study of this approach has not previously been reported.

As an extension of Xie et al. [187, 188], the transport of magnetic aerosols was considered using a CFD model in an alveolar bifurcation starting at the eighteenth respiratory generation, as shown in Figure 5, for a tracheal inhalation flow rate of 30 L/min. The aerosol was composed of 1 µm droplets containing 10% by mass magnetite nanoparticles. A permanent Alnico magnet was considered that had a wedge shaped design, as described in the study of Xie et al. [187], with a maximum strength of 0.4 Tesla and was positioned above the geometry 3 mm away from the wall surface. For the case of gravity acting on the aerosol without the magnetic force, the deposition fraction of the 1 µm aerosol was 0.5%. In contrast, the magnetic force was observed to increase the deposition fraction to 71.7% even though it was in the opposite direction of the gravity vector. Significantly stronger magnetic fields are needed to move the magnet further away from the geometry. However, these CFD results demonstrate how a simple permanent magnet can be used to target deposition within the alveolar region.

7. Discussion and Future Work

In conclusion, a variety of *in silico* models are available to simulate the delivery of aerosols to the respiratory tract. As expected, each of these models has inherent strengths and weaknesses. Both 1-D and 3-D CFD approaches have contributed to the current understanding of ambient aerosol transport and deposition in the respiratory airways. However, pharmaceutical aerosols often have the added complexities of spray momentum, turbulent inlet jets, and hygroscopic effects on droplet evaporation and condensational growth. As a result, the simulation of pharmaceutical aerosol delivery must often consider conditions from the site of aerosol formation in the inhaler to deposition within the respiratory airways. As reviewed, *in silico* models have developed to the point that they are now able to successfully predict transport and deposition of pharmaceutical aerosols in both the inhaler and respiratory airways providing good comparisons with *in vitro* and *in vivo* experimental data. Based on these successful validations, *in silico* models are now being used as a design tool to improve respiratory aerosol delivery and to potentially target the site of deposition. Specifically, models are currently being applied to (i) improve and optimize inhaler designs, (ii) specify design and usage parameters for improved delivery, (iii) propose new approaches for improved delivery to the lungs, and (iv) develop new methods to target the site of deposition within the respiratory airways. Applications reviewed in this study include the optimization of an existing spray inhaler design, development of charge-targeted delivery, the specification of conditions for optimal nasal delivery, advancement of the ECG concept for improved lung deposition, and an evaluation of targeted delivery using magnetic aerosols. It is expected that both 1-D whole-lung models and 3-D CFD simulations will play

an increasing role in improving the delivery of aerosols to the respiratory tract using many of the approaches described in this review.

Targeting the site of aerosol delivery to the respiratory tract is critical in many applications. Examples where effective targeted deposition is needed include the delivery of central nervous system medicines to the olfactory region of the nose, the delivery of inhaled chemotherapy agents, and the delivery of inhaled antibiotics. Kleinstreuer et al. [191] recently reviewed targeted aerosol deposition in the respiratory tract. In general, targeted delivery may refer to deposition in the lungs instead of the extrathoracic airways, deposition within a general region of the respiratory tract, such as the tracheobronchial or alveolar airways, or deposition at specific local sites such as a lung tumor or the olfactory region. Applications discussed in detail in this review focused on targeted delivery to the alveolar airways, lungs, and nasal cavity. In addition to these studies, Kleinstreuer et al. [10] proposed a method of highly localized targeting in which a spray is delivered to a small area of the mouth inlet. Using CFD simulations, the site of deposition can be determined allowing for the targeted delivery of drugs to specific areas, such as lung tumors. Tian et al. [35] showed that modifying the inlet temperature and relative humidity during ECG delivery affected deposition in the TB airways. For example, increasing the humidity temperature from 39 to 42 °C doubled the drug mass deposited in the first 7 branches of the conducting airways and maintained near zero MT deposition. While these results are promising, advancement of these methods as well as the development of new approaches are needed to better target the deposition of aerosols in the respiratory tract. This developmental process will clearly benefit from the application of advanced and validated CFD models.

Due to the complexity of both pharmaceutical delivery systems and deposition in the respiratory airways, validation of model results with experiments will remain a critical component of performing a thorough and reliable analysis. At a minimum, validations should compare with relevant existing *in vitro* and *in vivo* data sets. As described, improved experimental data sets are needed to better validate CFD predictions in local regions of the respiratory tract. Comparison of 3-D images of *in vivo* deposition with CFD simulations is a promising approach that should be pursued. However, in contrast with comparisons to preexisting studies, Longest and Hindle [42] describe the use of concurrent CFD modeling and *in vitro* experiments for the developed of delivery systems. In this approach, the *in vitro* experiments are used to determine initial aerosol conditions and benchmark the aerosol drug deposition performance of initial delivery systems. A validated CFD analysis of the system is then employed to describe the transport characteristics that are critical in the design of the system. The CFD results are used to quantify transport phenomena, like turbulence intensity, which influence inhaler mouthpiece drug deposition and the delivered dose to the patient. Quantitative correlations are potentially developed between inhaler design variables, the resulting transport characteristics, and performance endpoints. These correlations are then used in a design optimization process to quantitatively predict how changes in design will affect specific performance variables. Such an approach is consistent with the recent FDA quality by design (QbD) initiative in which a predictive understanding between cause and effect within an operating design space is highly desirable.

As described, a limitation of CFD models remains the computational cost such that only limited regions of the airway can be considered. To improve the simulation of transport dynamics throughout the airway, some studies have suggested combining CFD models of the upper airways with 1-D models of the lower airways [37, 192]. Lin et al. [37] resolved patient-specific dimensions of the entire TB airways from CT scans and illustrated a coupled 3-D and 1-D model. As an alternative approach, the use of individual paths as implemented by Tian et al. [35] may give a 3-D representation of transport from the mouth through the alveolar region. Tian et al. [35] described the use of individual paths to stochastically

characterize transport and deposition within the bifurcations of each lung lobe. Randomly generated individual path models are simulated to create an ensemble of deposition efficiencies. Averages of these ensemble results are then used to quantify transport conditions and deposition fractions (branch-averaged and highly localized) on a stochastic basis. This stochastic individual path (SIP) approach is essentially a 3-D application of the 1-D Monte Carlo method developed by Koblinger and Hofmann [95]. In addition to the deposition study of Tian et al. [35], Walters and Luke [193] recently showed that reduced path models of the TB airways had deposition characteristics similar to full models.

In summary, *in silico* models of aerosol transport are currently being applied to effectively improve the delivery of pharmaceutical aerosols and to target the site of aerosol deposition. Both 1-D and 3-D CFD models have been implemented to develop new drug delivery approaches, such as charge-targeted delivery and ECG. In general, model predictions are in agreement with available *in vitro* and *in vivo* data. However, more refined experimental data sets are needed to conduct more thorough validations of model performance, especially for highly localized deposition predictions. In terms of model development, future work remains in the areas of better validating localized predictions, developing more effective turbulence models, improving particle modeling efficiency, developing characteristic geometries of the airways, and developing stochastic 3-D representations of the airways like the proposed SIP model.

Acknowledgments

References

1. ICRP, Human Respiratory Tract Model for Radiological Protection. New York: Elsevier Science Ltd; 1994.

2. ICRP, Limits for Intakes of Radionuclides by Workers. Vol. 30. ICRP Publication; 1979. Part1

3. NCRP, Deposition, Retention and Dosimetry of Inhaled Radioactive Substances. Bethesda: National Council on Radiation Protection and Measurements; 1997.

4. Martonen TB. Mathematical model for the selective deposition of inhaled pharmaceuticals. Journal of Pharmaceutical Sciences. 1993; 82:1191–1199. [PubMed: 8308694]

5. Longest PW, Hindle M, Das Choudhuri S, Xi J. Comparison of ambient and spray aerosol deposition in a standard induction port and more realistic mouth-throat geometry. Journal of Aerosol Science. 2008; 39:572–591.

6. Longest PW, Hindle M, Das Choudhuri S. Effects of generation time on spray aerosol transport and deposition in models of the mouth-throat geometry. Journal of Aerosol Medicine and Pulmonary Drug Delivery. 2009; 22:67–84. [PubMed: 18956949]

7. DeHaan WH, Finlay WH. Predicting extrathoracic deposition from dry powder inhalers. Journal of Aerosol Science. 2004; 35:309–331.

8. Longest PW, Hindle M. CFD simulations of enhanced condensational growth (ECG) applied to respiratory drug delivery with comparisons to in vitro data. Journal of Aerosol Science. 2010; 41:805–820. [PubMed: 20835406]

9. Longest PW, Kleinstreuer C. Computational models for simulating multicomponent aerosol evaporation in the upper respiratory airways. Aerosol Science and Technology. 2005; 39:124–138.

10. Kleinstreuer C, Shi H, Zhang Z. Computational analyses of a pressurized metered dose inhaler and an new drug-aerosol targeting methodology. Journal of Aerosol Medicine. 2007; 20:294–309. [PubMed: 17894536]

11. Longest PW, Hindle M, Das Choudhuri S, Byron PR. Numerical simulations of capillary aerosol generation: CFD model development and comparisons with experimental data. Aerosol Science and Technology. 2007; 41:952–973.

12. Matida EA, Finlay WH, Breuer M, Lange CF. Improving prediction of aerosol deposition in an idealized mouth using large-eddy simulation. Journal of Aerosol Medicine. 2006; 19:290–300. [PubMed: 17034305]

13. Martonen, TB.; Burton, R.; Fleming, JS. 3D in silico modeling of aerosol behavior within airways of the human head and throat. Irvine, CA: Frontiers in Aerosol Dosimetry Research; 2005.

14. Isaacs, KK.; Rosati, JA.; Martonen, TB. Mechanisms of particle deposition. In: Ruzer, LS.; Harley, NH., editors. Aerosols Handbook. New York: CRC Press; 2005. p. 75-99.

15. Stahlhofen W, Rudolf G, James AC. Intercomparison of experimental regional aerosol deposition data. Journal of Aerosol Medicine. 1989; 2:285–308.

16. Finlay WH, Martin AR. Recent advances in predictive understanding of respiratory tract deposition. Journal of Aerosol Medicine and Pulmonary Drug Delivery. 2008; 21:189–205. [PubMed: 18518795]

17. Broday DM, Georgopoulous G. Growth and deposition of hygroscopic particulate matter in the human lung. Aerosol Science and Technology. 2001; 34:144–159.

18. Ferron GA, Oberdorster G, Hennenberg R. Estimation of the deposition of aerosolised drugs in the human respiratory tract due to hygroscopic growth. Journal of Aerosol Medicine. 1989; 2:271.

19. Bailey AG. The inhalation and deposition of charged particles within the human lung. Journal of Electrostatics. 1997; 42:25–32.

20. Martonen TB, Katz I. Deposition Patterns Of Polydisperse Aerosols Within Human Lungs. Journal Of Aerosol Medicine-Deposition Clearance And Effects In The Lung. 1993; 6:251–274.

21. Asgharian B, Hofmann W, Bergmann R. Particle deposition in a multiple-path model of the human lung. Aerosol Science and Technology. 2001; 34:332–339.

22. Ferziger, JH.; Peric, M. Computational Methods for Fluid Dynamics. Berlin: Springer-Verlag; 1999.

23. Wilcox, DC. Turbulence Modeling for CFD. 2nd Ed. California: DCW Industries, Inc; 1998.

24. Longest PW, Kleinstreuer C, Buchanan JR. Efficient computation of micro-particle dynamics including wall effects. Computers & Fluids. 2004; 33:577–601.

25. Longest PW, Xi J. Effectiveness of direct Lagrangian tracking models for simulating nanoparticle deposition in the upper airways. Aerosol Science and Technology. 2007; 41:380–397.

26. Longest PW, Oldham MJ. Numerical and experimental deposition of fine respiratory aerosols: Development of a two-phase drift flux model with near-wall velocity corrections. Aerosol Science. 2008; 39:48–70.

27. Xi J, Longest PW. Numerical predictions of submicrometer aerosol deposition in the nasal cavity using a novel drift flux approach. International Journal Of Heat And Mass Transfer. 2008; 51:5562–5577.

28. Xi J, Longest PW. Evaluation of a novel drift flux model for simulating submicrometer aerosol dynamics in human upper tracheobronchial airways. Annals of Biomedical Engineering. 2008; 36:1714–1734. [PubMed: 18712605]

29. Zhang Z, Kleinstreuer C. Airflow structures and nano-particle deposition in a human upper airway model. Journal of Computational Physics. 2004; 198:178–210.

30. Lambert AR, O'Shaughnessy PT, Tawhai MH, Hoffman EA, Lin C-L. Regional deposition of particles in an image-based airway model: Large-eddy simulation and left-right lung ventilation asymmetry. Aerosol Science and Technology. 2011; 45:11–25. [PubMed: 21307962]

31. Xi J, Longest PW. Transport and deposition of micro-aerosols in realistic and simplified models of the oral airway. Annals of Biomedical Engineering. 2007; 35:560–581. [PubMed: 17237991]

32. Longest PW, Vinchurkar S, Martonen TB. Transport and deposition of respiratory aerosols in models of childhood asthma. Journal of Aerosol Science. 2006; 37:1234–1257.

33. Zhang Z, Kleinstreuer C, Donohue JF, Kim CS. Comparison of micro- and nano-size particle depositions in a human upper airway model. Journal of Aerosol Science. 2005; 36:211–233.

34. Balashazy I, Hofmann W, Heistracher T. Computation of local enhancement factors for the quantification of particle deposition patterns in airway bifurcations. Journal of Aerosol Science. 1999; 30:185–203.

35. Tian G, Longest PW, Su G, Hindle M. Characterization of respiratory drug delivery with enhanced condensational growth (ECG) using an individual path model of the entire tracheobronchial airways. Annals of Biomedical Engineering. 2011; 39:1136–1153. [PubMed: 21152983]

36. Kleinstreuer C, Zhang Z. An adjustable triple-bifurcation unit model for air-particle flow simulations in human tracheobronchial airways. Journal of Biomechanical Engineering. 2009; 131:021007. [PubMed: 19102566]

37. Lin C-L, Tawhai MH, McLennan G, Hoffman EA. Multiscale simulation of gas flow in subject-specific models of the human lung. IEEE Engineering in Medicine and Biology. 2009; 28:25–33.

38. Phalen RF, Oldham MJ, Nel AE. Tracheobronchial particle dose considerations for in vitro toxicology studies. Toxicological Sciences. 2006; 92:126–132. [PubMed: 16597657]

39. Martonen TB, Musante CJ, Segal RA, Schroeter JD, Hwang D, Dolovich MA, Burton R, Spencer RM, Fleming JS. Lung Models: Strengths and Limitations. Respiratory Care. 2000; 45:712–736. [PubMed: 10894463]

40. Phalen RF, Mendez LB, Oldham MJ. New developments in aerosol dosimetry. Inhalation Toxicology. 2010

41. Coates MS, Chan H-K, Fletcher DF, Raper JA. Influence of air flow on the performance of a dry powder inhaler using computational and experimental analyses. Pharmaceutical Research. 2005; 22:1445–1453. [PubMed: 16132356]

42. Longest PW, Hindle M. Quantitative analysis and design of a spray aerosol inhaler. Part 1: Effects of dilution air inlets and flow paths. Journal of Aerosol Medicine and Pulmonary Drug Delivery. 2009; 22:271–283. [PubMed: 19466904]

43. Hindle M, Longest PW. Evaluation of enhanced condensational growth (ECG) for controlled respiratory drug delivery in a mouth-throat and upper tracheobronchial model. Pharmaceutical Research. 2010; 27:1800–1811. [PubMed: 20454837]

44. Chang, HK.; Paiva, M. Respiratory Physiology: An analytical approach. New York: Marcel Dekker; 1989.

45. Xi J, Longest PW, Martonen TB. Effects of the laryngeal jet on nano- and microparticle transport and deposition in an approximate model of the upper tracheobronchial airways. Journal of Applied Physiology. 2008; 104:1761–1777. [PubMed: 18388247]

46. Lin C-L, Tawhai MH, McLennan G, Hoffman EA. Characteristics of the turbulent laryngeal jet and its effect on airflow in the human intra-thoracic airways. Respiratory Physiology and Neurobiology. 2007; 157:295–309. [PubMed: 17360247]

47. Yu CP, Chandra K. Precipitation of submicron charged particles in human lung airways. Bull. Math. Biol. 1977; 39:471–478. [PubMed: 880411]

48. Robinson RJ, Yu CP. Coagulation of cigarette smoke particles. Journal of Aerosol Science. 1999; 30:533–548.

49. Yeh HC, Schum GM. Models of human lung airways and their application to inhaled particle deposition. Bull. Math. Biology. 1980; 42:461–480.

50. Goo J, Kim CS. Theoretical analysis of particle deposition in human lungs considering stochastic variations of airway morphology. Aerosol Science. 2003; 34:585–602.

51. Taulbee DB, Yu CP. A theory of aerosol deposition in the human respiratory tract. Journal Of Applied Physiology. 1975; 38:77–85. [PubMed: 1110247]

52. Matida EA, Finlay WH, Grgic LB. Improved numerical simulation of aerosol deposition in an idealized mouth-throat. Journal of Aerosol Science. 2004; 35:1–19.

53. Hofmann W, Sturm R, Fleming JS, Conway JH, Bolt L. Simulation of three-dimensional particle deposition patterns in human lungs and comparison with experimental SPECT data. Aerosol Science and Technology. 2005; 39:771–781.

54. Isaacs KK, Schlesinger RB, Martonen TB. Three-dimensional computational fluid dynamics simulations of particle deposition in the tracheobronchial tree. Journal of Aerosol Medicine. 2006; 19:344–352. [PubMed: 17034309]

55. Longest, PW.; Hindle, M.; Das Choudhuri, S.; Byron, PR. Developing a better understanding of spray system design using a combination of CFD modeling and experiment. In: Dalby, RN.; Byron, PR.; Peart, J.; Suman, JD.; Farr, SJ.; Young, PM., editors. Proceedings of Respiratory Drug Delivery 2008. Illinois: Davis Healthcare International Publishing; 2008. p. 151-163.

56. Wong W, Fletcher DF, Traini D, Chan HK, Crapper J, Young PM. Particle Aerosolisation and Break-up in Dry Powder Inhalers 1: Evaluation and Modelling of Venturi Effects for Agglomerated Systems. Pharmaceutical Research. 2010; 27:1367–1376. [PubMed: 20372989]

57. Longest PW, Hindle M. Evaluation of the Respimat Soft Mist inhaler using a concurrent CFD and in vitro approach. Journal of Aerosol Medicine and Pulmonary Drug Delivery. 2009; 22:99–112. [PubMed: 18956950]

58. Finlay WH, Martin AR. Modeling of aerosol deposition within interface devices. Journal of Aerosol Medicine. 2007; 20:S19–S28. [PubMed: 17411402]

59. Zhang Z, Kleinstreuer C. Low-Reynolds-number turbulent flows in locally constricted conduits: A comparison study. AIAA Journal. 2003; 41:831–840.

60. Liu Y, Matida EA, Gu J, Johnson MR. Numerical simulation of aerosol deposition in a 3-D human nasal cavity using RANS, RANS/EIM, and LES. Aerosol Science. 2007; 38:683–700.

61. Ilie M, Matida EA, Finlay WH. Asymmetrical aerosol deposition in an idealized mouth with a DPI mouthpiece inlet. Aerosol Science and Technology. 2008; 42:10–17.

62. Jin HH, Fan JR, Zeng MJ, Cen KF. Large eddy simulation of inhaled particle deposition within the human upper respiratory tract. Aerosol Science. 2007; 38:257–268.

63. Breuer M, Baytekin HT, Matida EA. Prediction of aerosol deposition in 90° bends using LES and an efficient Lagrangian tracking method. Journal of Aerosol Science. 2006; 37:1407–1428.

64. Kleinstreuer C, Zhang Z, Li Z. Modeling airflow and particle transport/deposition in pulmonary airways. Respiratory Physiology and Neurobiology. 2008; 163:128–138. [PubMed: 18674643]

65. Sznitman J, Heimshch T, Wildhaber JH, Tsuda A, Rosgen T. Respiratory flow phenomena and gravitational deposition in a three-dimensional space-filling model of the pulmonary acinar tree. Journal of Biomechanical Engineering. 2009; 131 031010-031011-031015.

66. Balashazy I, Hofmann W, Heistracher T. Local particle deposition patterns may play a key role in the development of lung cancer. Journal of Applied Physiology. 2003; 94:1719–1725. [PubMed: 12533493]

67. Comer JK, Kleinstreuer C, Hyun S, Kim CS. Aerosol transport and deposition in sequentially bifurcating airways. Journal of Biomechanical Engineering. 2000; 122:152–158. [PubMed: 10834155]

68. Comer JK, Kleinstreuer C, Kim CS. Flow structures and particle deposition patterns in double-bifurcation airway models. Part 2. Aerosol transport and deposition. Journal of Fluid Mechanics. 2001; 435:55–80.

69. Shi H, Kleinstreuer C, Zhang Z, Kim CS. Nanoparticle transport and deposition in bifurcating tubes with different inlet conditions. Physics of Fluids. 2004; 16:2199–2213.

70. Zhang Z, Kleinstreuer C, Kim CS. Cyclic micron-size particle inhalation and deposition in a triple bifurcation lung airway model. Journal of Aerosol Science. 2002; 33:257–281.

71. Balashazy, I.; Hofmann, W. Fluid dynamics and related particle deposition patterns in human airway bifurcations. In: Martonen, TB., editor. Medical Applications of Computer Modeling: The Respiratory System. Southampton: WIT Press; 2001. p. 83-108.

72. Longest PW, Vinchurkar S. Effects of mesh style and grid convergence on particle deposition in bifurcating airway models with comparisons to experimental data. Medical Engineering and Physics. 2007; 29:350–366. [PubMed: 16814588]

73. Longest PW, Xi J. Computational investigation of particle inertia effects on submicron aerosol deposition in the respiratory tract. Journal of Aerosol Science. 2007; 38:111–130.

74. Coates MS, Chan H-K, Fletcher DF, Chiou H. Influence of mouthpiece geometry on the aerosol delivery performance of a dry powder inhalation. Pharmaceutical Research. 2007; 24:1450–1456. [PubMed: 17404813]

75. Coates MS, Chan H-K, Fletcher DF, Raper JA. Effect of design on the performance of a dry powder inhaler using computational fluid dynamics. Part 2: Air inlet size. Journal of Pharmaceutical Sciences. 2006; 95:1382–1392. [PubMed: 16625656]

76. Coates MS, Fletcher DF, Chan H-K, Raper JA. Effect of design on the performance of a dry powder inhaler using computational fluid dynamics. Part 1: Grid structure and mouthpiece length. Journal of Pharmaceutical Sciences. 2004; 93:2863–2876. [PubMed: 15389665]

77. Wong W, Adi H, Traini D, Chan H-K, Fletcher DF, Crapper J, Young PM. Use of rapid prototyping and CFD in the design of DPI devices. Respiratory Drug Delivery. 2010; 2010:879–882.

78. Kroeger R, Becker M, Wynn E. Developments in techniques for simulation of particles in and from inhalers using CFD. Respiratory Drug Delivery Europe. 2010; 2009:231–234.

79. Dunbar CA, Watkins AP, Miller JF. An experimental investigation of the spray issued from a pMDI using laser diagnostic techniques. Journal of Aerosol Medicine. 1997; 10:351–368. [PubMed: 10175964]

80. Versteeg HK, Hargrave G, Harrington L, Shrubb I, Hodson D. The use of computational fluid dynamics (CFD) to predict pMDI air flows and aerosol plume formation. Respiratory Drug Delivery VII. 2000:257–264.

81. Stein SW, Gabrio BJ. Understanding throat deposition during cascade impactor testing. Respiratory Drug Delivery VII. 2000:287–290.

82. Cheng YS, Fu CS, Yazzie D, Zhou Y. Respiratory deposition patterns of salbutamol pMDI with CFC and HFA-134a formulations in a human airway replica. Journal of Aerosol Medicine. 2001; 14:255–266. [PubMed: 11681657]

83. Finlay, WH. The Mechanics of Inhaled Pharmaceutical Aerosols. San Diego: Academic Press; 2001.

84. Martonen, TB.; Rosati, JA.; Isaacs, KK. Modeling deposition of inhaled particles. In: Ruzer, LS.; Harley, NH., editors. Aerosols Handbook. New York: CRC Press; 2005. p. 113-155.

85. Ingham DB. Diffusion of aerosols from a stream flowing through a cylindrical tube. Journal of Aerosol Science. 1975; 6:125–132.

86. Rudolf G, Kobrich R, Stahlhofen W. Regional aerosol deposition in man-a statistical and algebraic model. Annals Of Occupational Hygiene. 1994; 38:1–14.

87. Kim CS, Jaques PA. Respiratory dose of inhaled ultrafine particles in healthy adults. Philosophical Transactions Of The Royal Society Of London Series A-Mathematical Physical And Engineering Sciences. 2000; 358:2693–2705.

88. Kim CS, Hu SC. Total respiratory tract depositon of fine micrometer-sized particles in healthy adults: emperical equations for sex and breathing pattern. Journal of Applied Physiology. 2006; 101:401–412. [PubMed: 16849812]

89. Martonen TB. Analytical model of hygroscopic particle behavior in human airways. Bulletin of Mathematical Biology. 1982; 44:425–442. [PubMed: 7104512]

90. Sbirlea-Apiou G, Lemaire M, Katz I, Conway J, Fleming JS, Martonen TB. Simulation of the regional manifestation of asthma. Journal of Pharmaceutical Sciences. 2004; 93:1205–1216. [PubMed: 15067697]

91. Martonen T, Fleming J, Schroeter J, Conway J, Hwang D. In silico modeling of asthma. Advanced Drug Delivery Reviews. 2003; 55:829–849. [PubMed: 12842603]

92. Phalen RF, Oldham MJ, Kleinman MT, Crocker TT. Tracheobronchial deposition predictions for infants, children and adolescents. Annals of Occupational Hygiene. 1988; 32:11–21.

93. Musante CJ, Martonen TB. Computer simulations of particle deposition in the developing human lung. Journal Of The Air & Waste Management Association. 2000; 50:1426–1432. [PubMed: 11002604]

94. Koblinger L, Hofmann W. Analysis of human lung morphometric data for stochastic aerosol deposition calculations. Phys. Med. Biol. 1985; 30:541–556. [PubMed: 4011676]

95. Koblinger L, Hofmann W. Monte Carlo modeling of aerosol deposition in human lungs. Part I: Simulation of particle transport in a stochastic lung structure. Journal of Aerosol Science. 1990; 21:661–674.

96. Hofmann W, Koblinger L. Monte-Carlo Modeling Of Aerosol Deposition In Human Lungs.3. Comparison With Experimental-Data. Journal Of Aerosol Science. 1992; 23:51–63.

97. Hofmann W, Asgharian B, Winkler-Heil R. Modeling intersubject variability of particle deposition in human lungs. Aerosol Science. 2002; 33:219–235.

98. Asgharian B, Price OT. Deposition of ultrafine (Nano) particles in the human lung. Inhalation Toxicology. 2007; 19:1045–1054. [PubMed: 17957545]

99. Asgharian B, Price OT. Airflow distribution in the human lung and its influence on particle deposition. Inhalation Toxicology. 2006; 18:795–801. [PubMed: 16774869]

100. Asgharian B, Price OT, Hofmann W. Prediction of particle deposition in the human lung using realistic models of lung ventilation. Aerosol Science. 2006; 37:1209–1221.

101. Schiller-Scotland CF, Hlawa R, Gebhart J. Experimental-Data For Total Deposition In The Respiratory-Tract Of Children. Toxicology Letters. 1994; 72:137–144. [PubMed: 8202925]

102. Kim CS. Deposition of aerosol particles in human lungs: in vivo measurement and modeling. Biomarkers. 2009; 14 S1:54–58. [PubMed: 19604060]

103. Fleming JS, Sauret V, Conway JH, Martonen TB. Validation of the conceptual anatomical model of the lung airway. Journal Of Aerosol Medicine-Deposition Clearance And Effects In The Lung. 2004; 17:260–269.

104. Fleming JS, Epps BP, Conway JH, Martonen TB. Comparison of SPECT aerosol deposition data with a human respiratory tract model. Journal Of Aerosol Medicine-Deposition Clearance And Effects In The Lung. 2006; 19:268–278.

105. Martin AR, Finlay WH. A general algebraic equation for predicting total respiratory tract deposition of micrometer-sized aerosol particles in humans. Journal Of Aerosol Science. 2007; 38:246–253.

106. Ferron GA. The size of soluable aerosol particles as a function of the humidity of the air: Application to the human respiratory tract. Journal of Aerosol Science. 1977; 3:251–267.

107. Finlay WH, Stapleton KW. The effect on regional lung deposition of coupled heat and mass-transfer between hygroscopic droplets and their surrounding phase. Journal of Aerosol Science. 1995; 26:655–670.

108. Finlay WH. Estimating the type of hygroscopic behavior exhibited by aqueous droplets. Journal of Aerosol Medicine. 1998; 11:221–229. [PubMed: 10346665]

109. Varghese SK, Gangamma S. Particle deposition in human respiratory system: Deposition of concentrated hygroscopic aerosols. Inhalation Toxicology. 2009; 21:619–630. [PubMed: 19459776]

110. Choi J, Kim CS. Mathematical analysis of particle deposition in human lungs: an improved single path transport model. Inhalation Toxicology. 2007; 19:925–939. [PubMed: 17849277]

111. Johnson DL, Martonen TB. Behavior Of Inhaled Fibers - Potential Applications To Medicinal Aerosols. Particulate Science And Technology. 1994; 12:161–173.

112. Park SS, Wexler AS. Particle deposition in the pulmonary region of the human lung: A semi-empirical model of single breath transport and deposition. Aerosol Science. 2007; 38:228–245.

113. Park SS, Wexler AS. Particle deposition in the pulmonary region of the human lung: Multiple breath aerosol transport and deposition. Journal Of Aerosol Science. 2007; 38:509–519.

114. Wilson IB. The deposition of charged aprticles in tubes, with reference to the retention of therapeutic aerosols in the human lung. J. Colloid. Sci. 1947; 2:271–276.

115. Vinchurkar S, Longest PW, Peart J. CFD simulations of the Andersen cascade impactor: Model development and effects of aerosol charge. Journal of Aerosol Science. 2009; 40:807–822.

116. Kwok PCL, Chan HK. Electrostatics of pharmaceutical inhalation aerosols. J. Pharm. Pharmacol. 2009; 61:1587–1599. [PubMed: 19958580]

117. Yu CP. Precipitation of unipolarly charged particles in cylindrical and spherical vessels. Journal of Aerosol Science. 1977; 8:237–241.

118. Thiagarajan V, Yu CP. Sedimentation from charged aerosol flows in parallel-plate and cylindrical channels. Journal of Aerosol Science. 1979; 10:405–410.

119. Chen YK, Yu CP. Particle deposition from duct flows by combined mechanisms. Aerosol Science and Technology. 1993; 19:389–395.

120. Balachandran W, Machowski W, Gaura E, Hudon C. Control of drug aerosol in human airways using electrostatic forces. Journal of Electrostatics. 1997; 40&41:579–584.

121. Bailey AG, Hashish AH, Williams TJ. Drug delivery by inhalation of charged particles. Journal of Electrostatics. 1998; 44:3–10.

122. Zimlich WC, Ding JY, Busick DR, Moutvic RR, Placke ME, Hirst PH, Pitcairn GR, Malik S, Newman S, Macintyre F, Miller PR, Shepheard MT, Lukas TM. The development of a novel electrohydrodynamic pulmonary drug delivery device. Respiratory Drug Delivery VII. 2000; 241–246

123. Borgstrom L, Olsson B, Thorsson L. Degree of throat deposition can explain the variability in lung deposition of inhaled drugs. Journal of Aerosol Medicine. 2006; 19:473–483. [PubMed: 17196076]

124. Kleinstreuer C, Zhang Z. Laminar-to-turbulent fluid-particle flows in a human airway model. International Journal Of Multiphase Flow. 2003; 29:271–289.

125. Cheng YS, Zhou Y, Chen BT. Particle deposition in a cast of human oral airways. Aerosol Science and Technology. 1999; 31:286–300.

126. Zhang Z, Kleinstreuer C. Species heat and mass transfer in a human upper airway model. International Journal of Heat and Mass Transfer. 2003; 46:4755–4768.

127. Sosnowski TR, Moskal A, Gradon L. Dynamics of oropharyngeal aerosol transport and deposition with the realistic flow pattern. Inhalation Toxicology. 2006; 18:773–780. [PubMed: 16774866]

128. Sosnowski TR, Moskal A, Gradon L. Mechanisms of aerosol particle deposition in the oro-pharynx under non-steady airflow. Annals of Occupational Hygiene. 2007; 51:19–25. [PubMed: 17041242]

129. Takano H, Nishida N, Itoh M, Hyo N, Majima Y. Inhaled particle deposition in unsteady-state respiratory flow at a numerically constructed model of the human larynx. Journal of Aerosol Medicine. 2006; 19:314–328. [PubMed: 17034307]

130. Jayaraju ST, Bronus M, Verbanck S, Lacor C. Fluid flow and particle deposition analysis in a realistic extrathoracic airway model using unstructured grids. Journal of Aerosol Science. 2007; 38:494–508.

131. Gemci T, Shortall B, Allen GM, Corcoran TE, Chigier N. A CFD study of the throat during aerosol drug delivery using heliox and air. Aerosol Science. 2003; 34:1175–1192.

132. Sandeau J, Katz I, Fodil R, Louis B, Apiou-Sbirlea G, Caillibotte G, Isabey D. CFD simulation of particle deposition in a reconstructed human oral extrathoracic airway for air and helium-oxygen mixtures. Journal Of Aerosol Science. 2010; 41:281–294.

133. Stapleton KW, Guentsch E, Hoskinson MK, Finlay WH. On the suitability of k-epsilon turbulence modeling for aerosol deposition in the mouth and throat: A comparison with experiment. Journal of Aerosol Science. 2000; 31:739–749.

134. Wang ZL, Grgic B, Finlay WH. A dry poweder inhaler with reduced mouth-throat deposition. Journal of Aerosol Medicine. 2006; 19:168–174. [PubMed: 16796541]

135. Grgic B, Finlay WH, Heenan AF. Regional aerosol deposition and flow measurements in an idealized mouth and throat. Aerosol Science. 2004; 35:21–32.

136. DeHaan WH, Finlay WH. In vitro monodisperse aerosol deposition in a mouth and throat with six different inhalation devices. Journal of Aerosol Medicine. 2001; 14:361–367. [PubMed: 11693848]

137. Zhang Y, Finlay WH, Matida EA. Particle deposition measurements and numerical simulations in a highly idealized mouth-throat. Journal of Aerosol Science. 2004; 35:789–803.

138. Zhang Y, Chia TL, Finlay WH. Experimental measurement and numerical study of particle deposition in highly idealized mouth-throat models. Aerosol Science and Technology. 2006; 40:361–372.

139. Xi J, Longest PW. Effects of oral airway geometry characteristics on the diffusional deposition of inhaled nanoparticles. ASME Journal of Biomechanical Engineering. 2008; 130:011008.

140. Grgic B, Finlay WH, Burnell PKP, Heenan AF. In vitro intersubject and intrasubject deposition measurements in realistic mouth-throat geometries. Journal of Aerosol Science. 2004; 35:1025–1040.

141. Matida EA, DeHaan WH, Finlay WH, Lange CF. Simulation of particle deposition in an idealized mouth with different small diameter inlets. Aerosol Science and Technology. 2003; 37:924–932.

142. Martonen TB, Zhang ZQ, Yue G, Musante CJ. Fine particle deposition within human nasal airways. Inhalation Toxicology. 2003; 15:283–303. [PubMed: 12635000]

143. Shi H, Kleinstreuer C, Zhang Z. Laminar airflow and nanoparticle or vapor deposition in a human nasal cavity model. Journal of Biomechanical Engineering. 2006; 128:697–706. [PubMed: 16995756]

144. Zamankhan P, Ahmadi G, Wang Z, Hopke PK, Cheng YS, Su WC, Leonard D. Airflow and deposition of nano-particles in a human nasal cavity. Aerosol Science and Technology. 2006; 40:463–476.

145. Cheng KH, Cheng YS, Yeh HC, Guilmette RA, Simpson SQ, Yang SQ, Swift DL. In vivo measurements of nasal airway dimensions and ultrafine aerosol depositing in human nasal and oral airways. Journal of Aerosol Science. 1996; 27:785–801.

146. Schroeter JD, Kimbell JS, Asgharian B. Analysis of particle deposition in the turbinate and olfactory regions using a human nasal computational fluid dynamics model. Journal of Aerosol Medicine. 2006; 19:301–313. [PubMed: 17034306]

147. Shi H, Kleinstreuer C, Zhang Z. Modeling of inertial particle transport and deposition in human nasal cavities with wall roughness. Aerosol Science. 2007; 38:398–419.

148. Shanley KT, Zamankhan P, Ahmadi G, Hopke PK, Cheng YS. Numerical Simulations Investigating the Regional and Overall Deposition Efficiency of the Human Nasal Cavity. Inhalation Toxicology. 2008; 20:1093–1100. [PubMed: 18800272]

149. Schroeter JD, Garcia GJM, Kimbell JS. Effects of surface smoothness on inertial particle deposition in human nasal models. Journal of Aerosol Science. 2011; 42:52–63. [PubMed: 21339833]

150. Schroeter JD, Musante CJ, Hwang DM, Burton R, Guilmette R, Martonen TB. Hygroscopic growth and deposition of inhaled secondary cigarette smoke in human nasal pathways. Aerosol Science and Technology. 2001; 34:137–143.

151. Kimbell JS, Segal RA, Asgharian B, Wong BA, Schroeter JD, Southall JP, Dickens CJ, Brace G, Miller FJ. Characterization of deposition from nasal spray devices using a computational fluid dynamics model of the human nasal passages. Journal Of Aerosol Medicine-Deposition Clearance And Effects In The Lung. 2007; 20:59–74.

152. Longest PW, Tian G, Hindle M. Improving the lung delivery of nasally administered aerosols during noninvasive ventilation - An application of enhanced condensational growth (ECG). Journal of Aerosol Medicine and Pulmonary Drug Delivery. 2011; 24:103–118. [PubMed: 21410327]

153. Foo MY, Cheng YS, Su WC, Donovan MD. The influence of spray properties on intranasal deposition. Journal of Aerosol Medicine. 2007; 20:495–508. [PubMed: 18158721]

154. Kim CS, Fisher D. Deposition characteristics of aerosol particles in sequentially bifurcating airway models. Aerosol Science and Technology. 1999; 31:198–220.

155. Zhang Z, Kleinstreuer C. Effect of particle inlet distributions on deposition in a triple bifurcation lung airway model. Journal of Aerosol Medicine-Deposition Clearance and Effects In The Lung. 2001; 14:13–29.

156. Zhang Z, Kleinstreuer C, Kim CS. Flow structure and particle transport in a triple bifurcation airway model. Journal of Fluids Engineering-Transactions of the ASME. 2001; 123:320–330.

157. Longest PW, Vinchurkar S. Validating CFD predictions of respiratory aerosol deposition: effects of upstream transition and turbulence. Journal of Biomechanics. 2007; 40:305–316. [PubMed: 16533511]

158. Oldham MJ, Phalen RF, Heistracher T. Computational fluid dynamic predictions and experimental results for particle deposition in an airway model. Aerosol Science and Technology. 2000; 32:61–71.

159. Longest PW, Oldham MJ. Mutual enhancements of CFD modeling and experimental data: A case study of one micrometer particle deposition in a branching airway model. Inhalation Toxicology. 2006; 18:761–772. [PubMed: 16774865]

160. Oldham MJ. Challenges in validating CFD-derived inhaled aerosol deposition predictions. Inhalation Toxicology. 2006; 18:781–786. [PubMed: 16774867]

161. Robinson RJ, Oldham MJ, Clinkenbeard RE, Rai P. Experimental and numerical smoke carcinogen deposition in a multi-generation human replica tracheobronchial model. Annals of Biomedical Engineering. 2006; 34:373–383. [PubMed: 16456639]

162. Cohen BS, Sussman RG, Lippmann M. Ultrafine particle deposition in a human tracheobronchial cast. Aerosol Science and Technology. 1990; 12:1082–1093.

163. Gurman JL, Lippmann M, Schlesinger RB. Particle deposition in replicate casts of the human upper trancheobronchial tree under constant and cyclic inspiratory flow. I. Experimental. Aerosol Science and Technology. 1984; 3:245–252.

164. Martonen, TB. Surrogate experimental models for studying particle deposition in the human respiratory tract: An overview. In: Lee, SD., editor. Aerosols. Chesea, Michigan: Lewis Publishers; 1986.

165. Vinchurkar S, Longest PW. Evaluation of hexahedral, prismatic and hybrid mesh styles for simulating respiratory aerosol dynamics. Computers and Fluids. 2008; 37:317–331.

166. Jayaraju ST, Brouns M, Lacor C, Belkassem B, Verbanck S. Large eddy and detached eddy simulations of fluid flow and particle deposition in a human mouth-throat. Aerosol Science. 2008; 39:862–875.

167. Li Z, Kleinstreuer C, Zhang Z. Particle deposition in the human tracheobronchial airways due to transient inspiratory flow patterns. Aerosol Science. 2007; 38:625–644.

168. Ma B, Lutchen KR. CFD simulations of aeroosl depostion in an anatomically based human large-medium airway model. Annals of Biomedical Engineering. 2009; 37:271–285. [PubMed: 19082892]

169. Gemci T, Ponyavin V, Chen Y, Chen H, Collins R. Computational model of airflow in upper 17 generations of human respiratory tract. Journal of Biomechanics. 2008; 41:2047–2054. [PubMed: 18501360]

170. Zhang Z, Kleinstreuer C, Kim CS. Comparison of analytical and CFD models with regard to micron particle deposition in a human 16-generation tracheobronchial airway model. Aerosol Science. 2009; 40:16–28.

171. Longest PW, Xi J. Condensational growth may contribute to the enhanced deposition of cigarette smoke particles in the upper respiratory tract. Aerosol Science and Technology. 2008; 42:579–602.

172. Zhang Z, Kleinstreuer C, Kim CS. Isotonic and hypertonic saline droplet deposition in a human upper airway model. Journal of Aerosol Medicine. 2006; 19:184–198. [PubMed: 16796543]

173. Longest PW, McLeskey JT, Hindle M. Characterization of nanoaerosol size change during enhanced condensational growth. Aerosol Science and Technology. 2010; 44:473–483. [PubMed: 20640054]

174. Kumar H, Tawhai MH, Hoffman EA, Lin C-L. The effects of geometry on airflow in the acinar region of the human lung. Journal of Biomechanics. 2009; 42:1635–1642. [PubMed: 19482288]

175. Berg EJ, Weisman JL, Oldham MJ, Robinson RJ. Flow field analysis in a compliant acinus replica model using particle image velocimetry (PIV). Journal of Biomechanics. 2010; 43:1039–1047. [PubMed: 20116064]

176. Kojic M, Tsuda A. A simple model for gravitational deposition of non-diffusing particles in oscillatory laminar pipe flow and its application to small airways. Journal of Aerosol Science. 2004; 35:245–261.

177. Haber S, Butler JP, Brenner H, Emanuel I, Tsuda A. Shear flow over a self-similar expanding pulmonary alveolus during rhythmical breathing. Journal of Fluid Mechanics. 2000; 405:243–268.

178. Schirrmann K, Mertens M, Kertzscher U, Kuebler WM, Affeld K. Theoretical modeling of the interaction between alveoli during inflation and deflation in normal and diseased lungs. Journal of biomechanics. 2010; 43:1202–1207. [PubMed: 20031137]

179. Haber S, Yitzhak D, Tsuda A. Gravitational deposition in a rhythmically expanding and contracting alveolus. Journal of Applied Physiology. 2003; 95:657–671. [PubMed: 12639848]

180. Ardila R, Horie T, Hildebrandt J. Macroscopic isotropy of lung expansion. Respiration Physiology. 1974; 20:105–115. [PubMed: 4826745]

181. Tsuda A, Rogers RA, Hydon PE, Butler JP. Chaotic mixing deep in the lung. Proceedings of the National Academy of Sciences of the United States of America. 2002; 99:10173–10178. [PubMed: 12119385]

182. Balashazy I, Hofmann W, Farkas A, Madas BG. Three-Dimensional Model for Aerosol Transport and Deposition in Expanding and Contracting Alveoli. Inhalation Toxicology. 2008; 20:611–621. [PubMed: 18444013]

183. Darquenne C, Paiva M. Two- and three-dimensional simulations of aerosol transport and deposition in alveolar zone of human lung. Journal of Applied Physiology. 1996; 80:1401–1414. [PubMed: 8926273]

184. Lee DY, Lee JW. Characteristics of particle transport in an expanding or contracting alveolated tube. Journal of Aerosol Science. 2003; 34:1193–1215.

185. Tsuda A, Henry FS, Butler JP. Chaotic mixing of alveolated duct flow in rhythmically expanding pulmonary acinus. Journal of Applied Physiology. 1995; 79:1055–1063. [PubMed: 8567502]

186. Dailey HL, Ghadiali SN. Fluid-structure analysis of microparticle transport in deformable pulmonary alveoli. Journal of Aerosol Science. 2007; 38:269–288.

187. Xie Y, Zeng P, Siegel R, Wiedmann TS, Hammer BE, Longest PW. Magnetic deposition of aerosols composed of aggregated superparamagnetic nanoparticles. Pharmaceutical Research. 2010; 27:855–865. [PubMed: 20198407]

188. Xie YY, Longest PW, Xu YH, Wang JP, Wiedmann TS. In vitro and in vivo lung deposition of coated magnetic aerosol particles. Journal of Pharmaceutical Sciences. 2010; 99:4658–4668. [PubMed: 20845463]

189. Martin AR, Finlay WH. Magnetic alignment of aerosol particles for targeted pulmonary drug delivery: Comparison of magnetic and aerodynamic torques. J. Comput. Theor. Nanosci. 2008; 5:2067–2070.

190. Redman GES, Martin AR, Waszak P, Thompson RB, Cheung PY, Thebaud B, Finlay WH. Pilot study of inhaled aerosols targeted via magnetic alignment of high aspect ratio particles in rabbits. J. Nanomater. 2011; 130721

191. Kleinstreuer C, Zhang Z, Donohue JF. Targeted drug-aerosol delivery in the human respiratory system. Annu. Rev. Biomed. Eng. 2008; 10:195–220. [PubMed: 18412536]

192. 2005. COPHIT, http://www-waterloo.ansys.com/cfx/European_Projects/cophit

193. Walters DK, Luke WH. Computational fluid dynamics simulations of particle deposition in large-scale multigenerational lung models. Journal Of Biomechanical Engineering. 2011; 133:011003. [PubMed: 21186893]
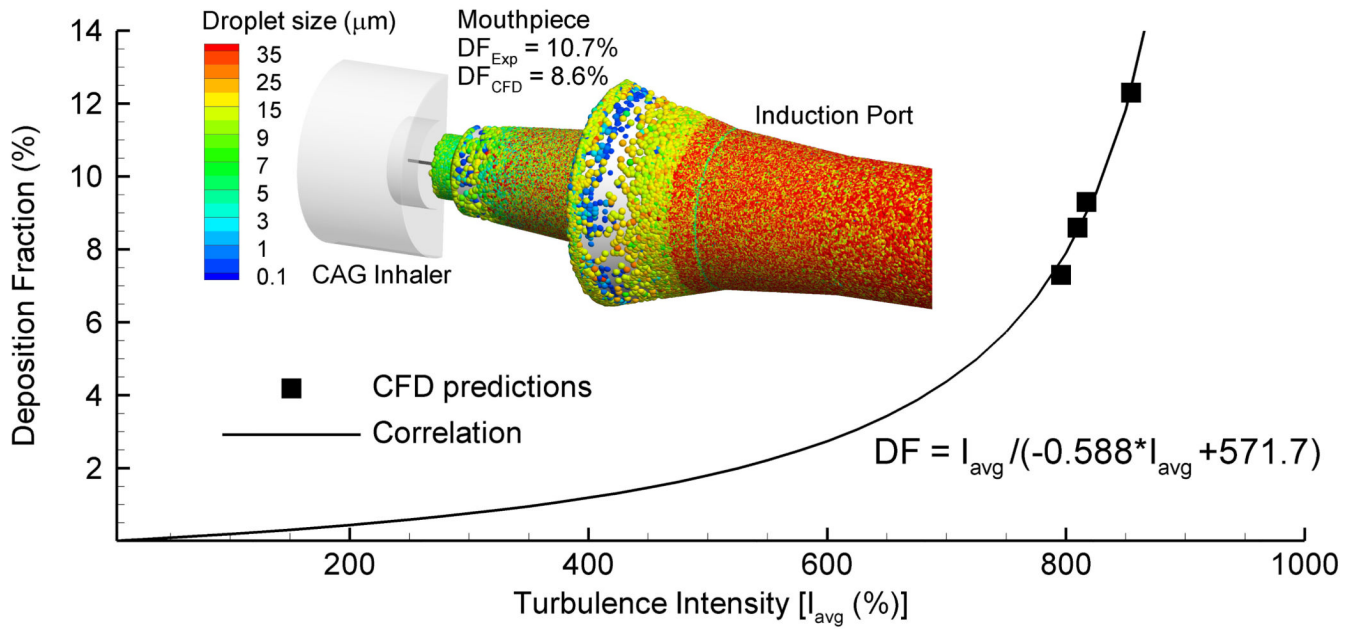
The chart shows a plot with axes: Deposition Fraction (%) on the y-axis (0–14) and Turbulence Intensity [I_{avg} (%)] on the x-axis (200–1000). Legend includes:

- Droplet size (μm): 35, 25, 15, 9, 7, 5, 3, 1, 0.1
- Mouthpiece: DF_{Exp} = 10.7%, DF_{CFD} = 8.6%
- Induction Port
- CAG Inhaler
- ■ CFD predictions
- — Correlation

$$DF = I_{avg}/(-0.588 * I_{avg} + 571.7)$$

Figure 1.
Deposition fraction (DF) as a function of average turbulence intensity (I_{avg}) for a prototype capillary aerosol generator (CAG). The insert shows the inhaler body, heated microcapillary, and prototype mouthpiece connected to an induction port. Predicted deposition fractions between the experiment (Exp) and CFD model were in close agreement. The developed correlation can be used to optimize the inhaler design to minimize mouthpiece deposition, as described by Longest and Hindle [42].
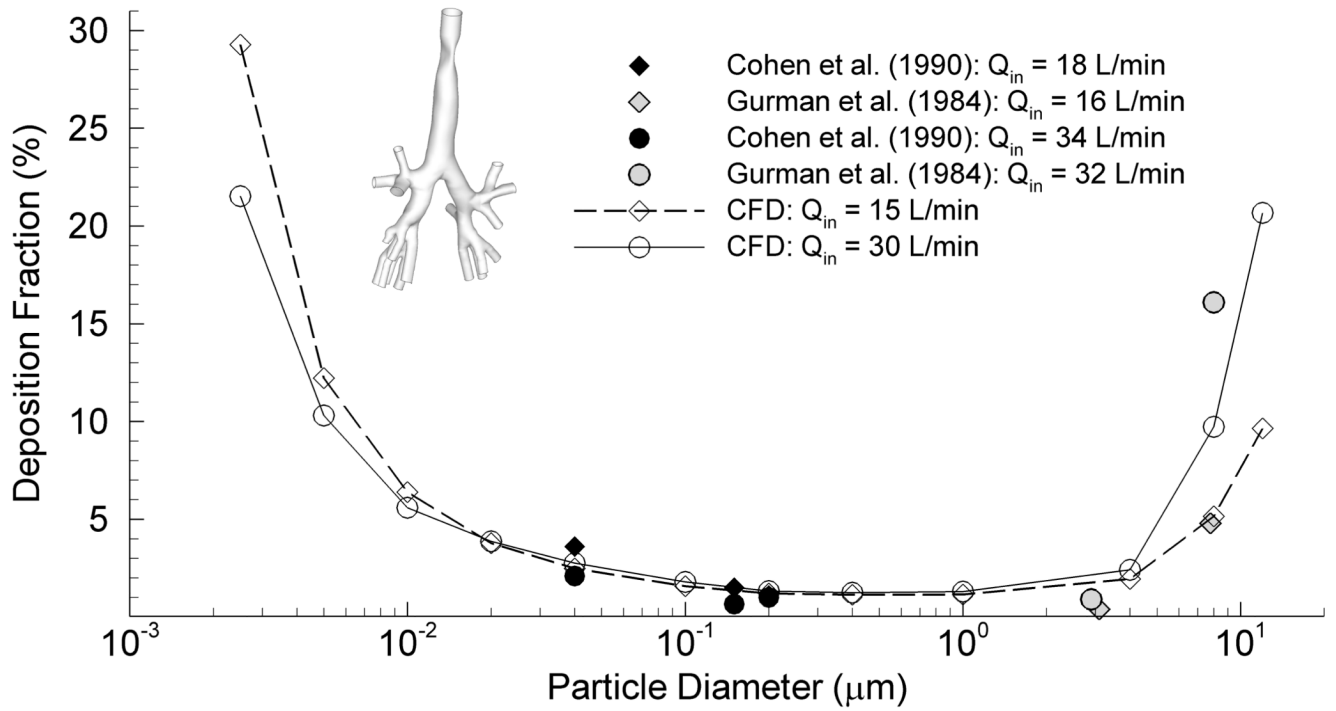
Figure 2.
Comparison of CFD model predictions and experimental results of deposition fraction in a
TB model of the upper conducting airways. The original cast used in the experimental
studies was obtained and scanned to produce the geometric model (see insert) and CFD
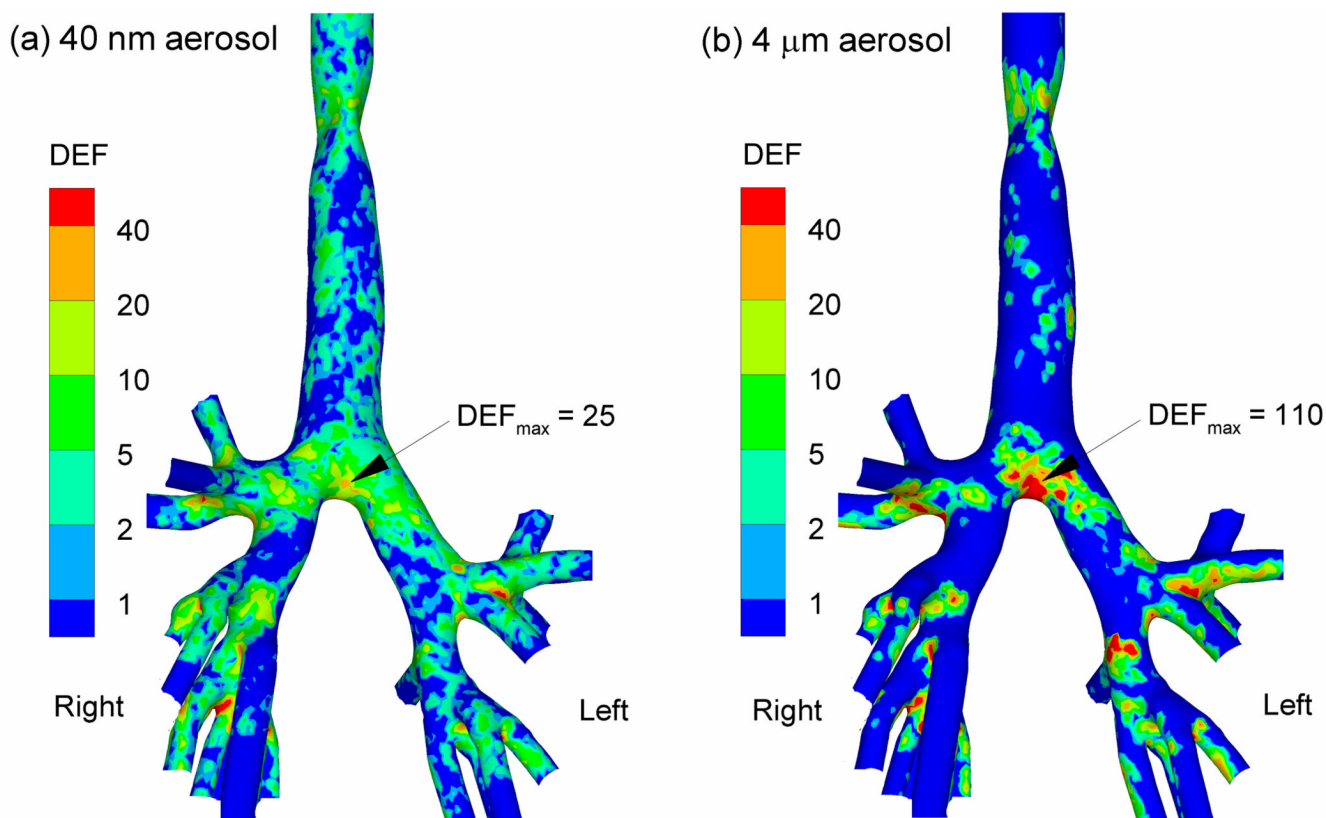results, as described by Xi et al. [45].

Figure 3.
Deposition enhancement factors (DEFs) for a steady state inhalation flow rate of 30 L/min in a cast-based model of the upper TB airways with particle sizes of (a) 40 nm and (b) 4 µm. DEF values represent the ratio of locally deposited mass to total deposited mass in the airway. Significant enhancement in local deposition is observed for both nanometer (factor of 25) and micrometer (factor of 110) aerosols.
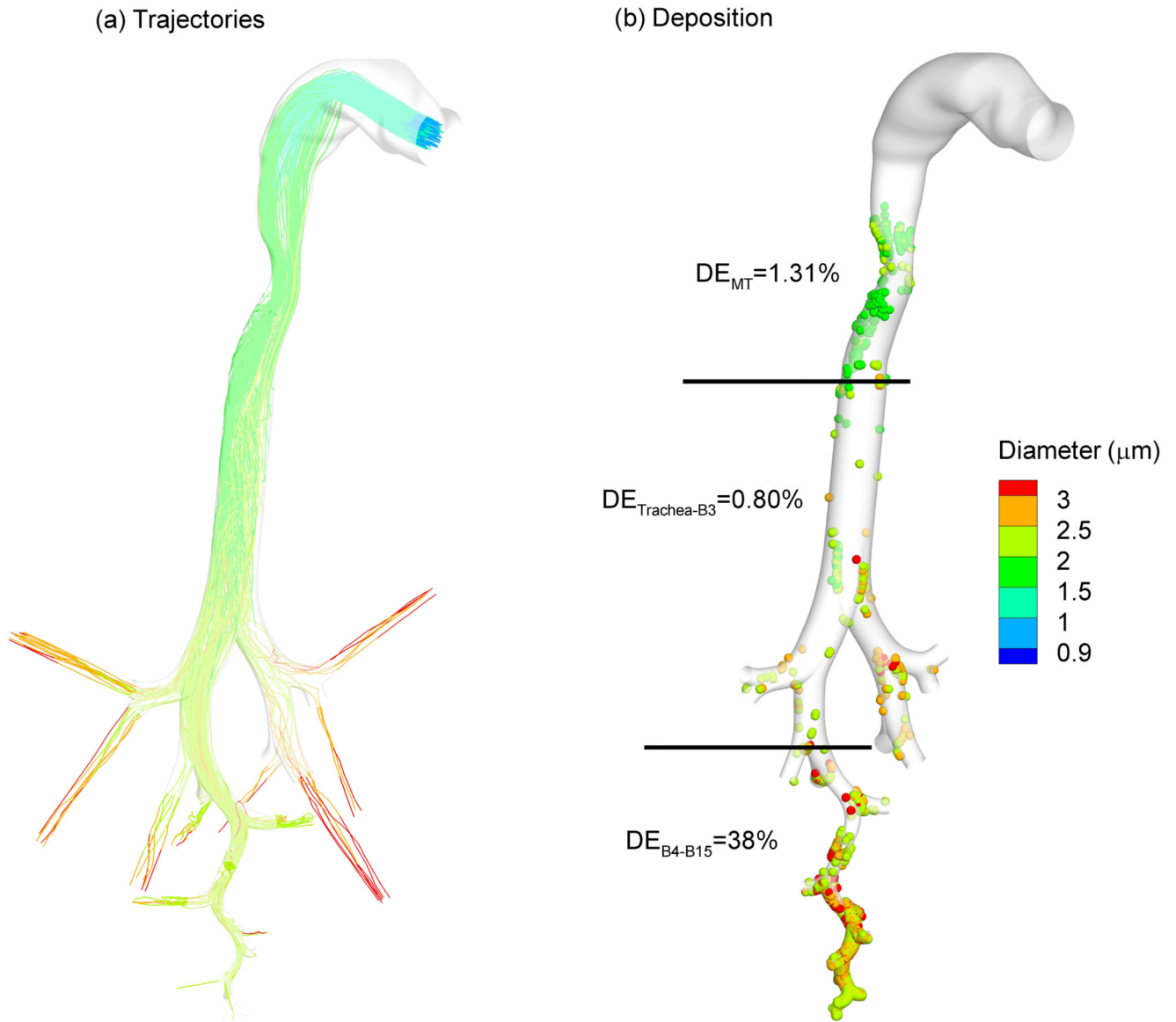
(a) Trajectories

(b) Deposition

DE_{MT}=1.31%

$DE_{Trachea-B3}$=0.80%

DE_{B4-B15}=38%

Diameter (µm)
- 3
- 2.5
- 2
- 1.5
- 1
- 0.9

Figure 4.
Enhanced condensational growth (ECG) delivery of an initially 900 nm aerosol with a humidity stream temperature of 39 °C in terms of (a) trajectories and (b) deposition locations contoured according to droplet size. For this delivery condition, growth from 900 nm to approximately 2.5 µm is observed, which results in significant deposition in the lower TB airways. Tian et al. [35] showed that near full retention of the aerosol occurs in the alveolar region.
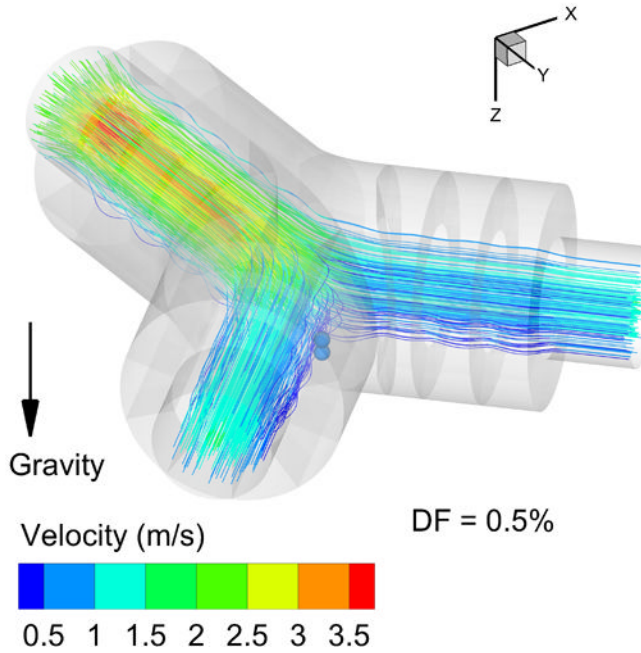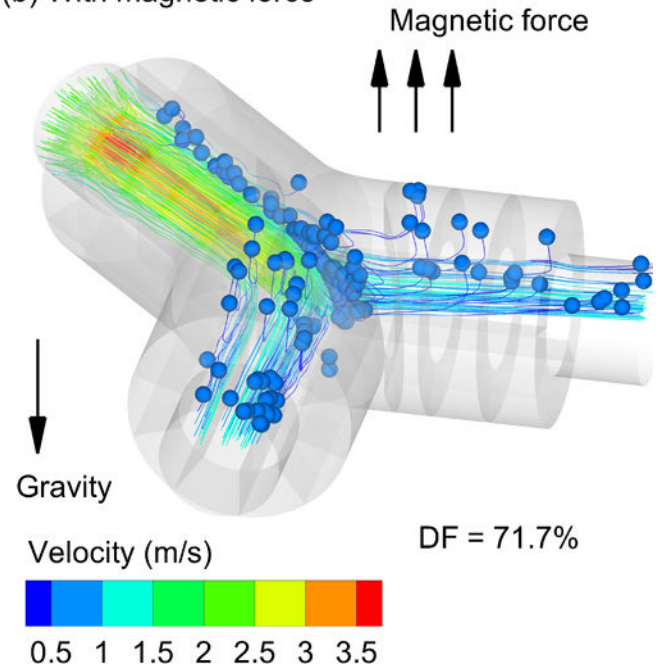
Figure 5.
Transport and deposition of magnetic aerosols in a model of an alveolar bifurcation starting at generation 17 at a tracheal flow rate of 30 L/min under the action of (a) gravity and (b) gravity and a magnetic force. The aerosol was composed of 1 µm droplets containing 10% by mass magnetite nanoparticles. The magnetic force is shown to significantly influence the deposition of the aerosol.